



NAVAL POSTGRADUATE SCHOOL

MONTEREY, CALIFORNIA

THESIS

**FLUID STRUCTURE INTERACTION EFFECTS ON
COMPOSITES UNDER LOW VELOCITY IMPACT**

by

Ryan P. Conner
June 2012

Thesis Advisor:
Second Reader:

Young W. Kwon
Jarema M. Didoszak

Approved for public release; distribution is unlimited.

THIS PAGE INTENTIONALLY LEFT BLANK

REPORT DOCUMENTATION PAGE			<i>Form Approved OMB No. 0704-0188</i>	
Public reporting burden for this collection of information is estimated to average 1 hour per response, including the time for reviewing instruction, searching existing data sources, gathering and maintaining the data needed, and completing and reviewing the collection of information. Send comments regarding this burden estimate or any other aspect of this collection of information, including suggestions for reducing this burden, to Washington headquarters Services, Directorate for Information Operations and Reports, 1215 Jefferson Davis Highway, Suite 1204, Arlington, VA 22202-4302, and to the Office of Management and Budget, Paperwork Reduction Project (0704-0188) Washington DC 20503.				
1. AGENCY USE ONLY (Leave blank)		2. REPORT DATE June 2012	3. REPORT TYPE AND DATES COVERED Master's Thesis	
4. TITLE AND SUBTITLE Fluid Structure Interaction Effects on Composites Under Low Velocity Impact			5. FUNDING NUMBERS	
6. AUTHOR(S) Ryan Conner				
7. PERFORMING ORGANIZATION NAME(S) AND ADDRESS(ES) Naval Postgraduate School Monterey, CA 93943-5000			8. PERFORMING ORGANIZATION REPORT NUMBER	
9. SPONSORING /MONITORING AGENCY NAME(S) AND ADDRESS(ES) N/A			10. SPONSORING/MONITORING AGENCY REPORT NUMBER	
11. SUPPLEMENTARY NOTES The views expressed in this thesis are those of the author and do not reflect the official policy or position of the Department of Defense or the U.S. Government. IRB Protocol number _____ N/A _____.				
12a. DISTRIBUTION / AVAILABILITY STATEMENT Approved for public release; distribution is unlimited.			12b. DISTRIBUTION CODE	
13. ABSTRACT (maximum 200 words) <p>In this study composite materials were tested in different fluid environments to determine the role of Fluid Structure Interaction with these composites under a lower velocity impact. The purpose of this research is to develop a better understanding of possible marine applications of composite materials.</p> <p>This was done using a low velocity impact machine and two composite types. The first composite is made from a multi-ply symmetrical plain weave 6 oz. E-glass skin. The test area of the composites is 12 in by 12 in (30.5 cm by 30.5 cm) with clamped boundary conditions. The testing was done using a drop weight system to impact the center of the test area. A Plexiglas box in conjunction with the impact machine was used to keep the top of the composite sample dry while it was submerged in approximately 15 inches (38.10 cm) of water.</p> <p>The second composite type was constructed using the same methods, but was made from a Carbon Fiber Reinforced Polymer (CFRP) instead of the E-glass skin. These samples were pre-cracked and tested using the same impact machine in 15 inches (38.10 cm) of water. The overall size of these samples was 42 cm long and 3 cm wide forming a long thin rectangular shape. The test area of these samples was a 20 cm long section of the sample with the outsides being clamped to achieve the desired boundary conditions. Two variations of these samples were tested. The first was reinforced with Multi-Walled Carbon Nanotubes (MWCNTs) and the second had no reinforcements at the interface layer in front of the pre-cracks. Output from both tests was recorded using strain gauges and a force impact sensor. The results show that an added mass from the water plays a large role in the Fluid Structure Interaction with composites due to the similar densities of water and the composites.</p>				
14. SUBJECT TERMS Composites, Fluid Structure Interaction, FSI, low velocity impact, carbon fiber reinforced polymers, CFRP, carbon nanotubes, CNT, vacuum assisted resin transfer molding, VARTM.			15. NUMBER OF PAGES 77	
			16. PRICE CODE	
17. SECURITY CLASSIFICATION OF REPORT Unclassified	18. SECURITY CLASSIFICATION OF THIS PAGE Unclassified	19. SECURITY CLASSIFICATION OF ABSTRACT Unclassified	20. LIMITATION OF ABSTRACT UU	

THIS PAGE INTENTIONALLY LEFT BLANK

Approved for public release; distribution unlimited.

**FLUID STRUCTURE INTERACTION EFFECTS ON COMPOSITES UNDER
LOW VELOCITY IMPACT**

Ryan P. Conner
Lieutenant, United States Navy
B.S., Virginia Tech, 2008

Submitted in partial fulfillment of the
requirements for the degree of

MASTER OF SCIENCE IN MECHANICAL ENGINEERING

from the

**NAVAL POSTGRADUATE SCHOOL
June 2012**

Author: Ryan P. Conner

Approved by: Young W. Kwon
Thesis Advisor

Jarema M. Didoszak
Second Reader

Knox T. Millsaps
Chair, Department of Mechanical and Aerospace Engineering

THIS PAGE INTENTIONALLY LEFT BLANK

ABSTRACT

In this study composite materials were tested in different fluid environments to determine the role of Fluid Structure Interaction with these composites under a lower velocity impact. The purpose of this research is to develop a better understanding of possible marine applications of composite materials.

This was done using a low velocity impact machine and two composite types. The first composite is made from a multi-ply symmetrical plain weave 6 oz. E-glass skin. The test area of the composites is 12 in by 12 in (30.5 cm by 30.5 cm) with clamped boundary conditions. The testing was done using a drop weight system to impact the center of the test area. A Plexiglas box in conjunction with the impact machine was used to keep the top of the composite sample dry while it was submerged in approximately 15 inches (38.10 cm) of water.

The second composite type was constructed using the same methods, but was made from a Carbon Fiber Reinforced Polymer (CFRP) instead of the E-glass skin. These samples were pre-cracked and tested using the same impact machine in 15 inches (38.10 cm) of water. The overall size of these samples was 42 cm long and 3 cm wide forming a long thin rectangular shape. The test area of these samples was a 20 cm long section of the sample with the outsides being clamped to achieve the desired boundary conditions. Two variations of these samples were tested. The first was reinforced with Multi-Walled Carbon Nanotubes (MWCNTs) and the second had no reinforcements at the interface layer in front of the pre-cracks. Output from both tests was recorded using strain gauges and a force impact sensor. The results show that an added mass from the water plays a large role in the Fluid Structure Interaction with composites due to the similar densities of water and the composites.

THIS PAGE INTENTIONALLY LEFT BLANK

TABLE OF CONTENTS

I.	INTRODUCTION.....	1
A.	BACKGROUND.....	1
	1. Composites.....	1
	2. Fluid Structure Interaction.....	1
B.	OBJECTIVES	2
II.	EXPERIMENTAL METHODS FOR E-GLASS COMPOSITE	5
A.	MATERIALS	5
	1. E-Glass	5
	2. Vinyl Ester Resin.....	6
	3. Hardening Agents for Resin.....	6
	a. Methyl Ethyl Ketone Peroxide	6
	b. Cobalt Naphthenate	7
	c. Dimethylaniline.....	8
B.	COMPOSITE CONSTRUCTION METHOD	8
	1. Vacuum Assisted Resin Transfer Molding.....	8
	2. Materials	9
	3. Procedure.....	9
	a. Preparation and Layup	9
	b. Resin Preparation	12
C.	POST FABRICATION METHODS AND REQUIREMENTS.....	13
	1. Curing	13
	2. Sizing	14
	3. Strain Gages	14
	a. Overview	15
	b. Application to Composites	15
D.	TEST EQUIPMENT.....	16
E.	TEST METHODS.....	17
	1. E-Glass Composite Sample	17
	a. Setup	18
	b. Drop Weight and Drop Heights.....	20
	2. Carbon Fiber Reinforced Polymer Sample	21
III.	RESULTS AND ANALYSIS	25
A.	E-GLASS COMPOSITE	25
	1. Overview	25
	2. Force Analysis	27
	3. Strain Analysis	34
B.	CARBON FIBER REINFORCED POLYMER COMPOSITE	39
	1. Overview	39
	2. Force Analysis	39
	3. Strain Analysis	48
IV.	CONCLUSION	53

V. RECOMMENDED FURTHER STUDY	55
LIST OF REFERENCES.....	57
INITIAL DISTRIBUTION LIST	59

LIST OF FIGURES

Figure 1.	Six ounce E-Glass weave.....	5
Figure 2.	Methyl Ethyl Ketone Peroxide (MEKP).....	7
Figure 3.	Bottle of Cobalt.....	7
Figure 4.	Bottle of Dimethylaniline (DMA).	8
Figure 5.	Final product of preform layup.....	10
Figure 6.	Preform Layup [11].....	11
Figure 7.	Comparing the flexible tubing to the stiff tubing.....	12
Figure 8.	Square strain gage rosette showing ϵ_1 , ϵ_2 , ϵ_3	14
Figure 9.	Strain Gage layout on composite samples.	15
Figure 10.	M-bond AE-10 strain gage adhesive [13].	16
Figure 11.	Impact test machine.	17
Figure 12.	Plexiglas box used to keep the top of the composite dry while being submerged in a water filled tank.	19
Figure 13.	New setup using expanding spray foam as a second layer of water proofing.....	20
Figure 14.	Bonded Strain Gage [5].	22
Figure 15.	CFRP coupons sandwiched between two aluminum plates [5].	22
Figure 16.	CFRP coupon dimensions.....	23
Figure 17.	CFRP coupon clamped and ready for water testing.....	24
Figure 18.	Delamination under impact zone of wet sample.....	26
Figure 19.	Close up of delamination under impact zone of wet sample.	26
Figure 20.	Force comparison of 12.70 cm (5in) drop height dry testing.	27
Figure 21.	Force comparison of 12.70 cm (5in) drop height for wet testing.	28
Figure 22.	Force comparison of 30.48 cm (12in) drop height dry testing.	28
Figure 23.	Force comparison of 30.48 cm (12in) drop height for wet testing.	29
Figure 24.	Impact force comparison between wet and dry testing with drop height of 15.24 cm (6 in).....	30
Figure 25.	Damage as a function of drop height for both wet and dry samples.....	31
Figure 26.	Impact force comparison showing same impact force due to damage in wet sample with a drop height of 20.32 cm (8 in).	32
Figure 27.	Impact force comparison showing the dry force still larger than the wet force, but smaller difference at 50.80 cm (20 in) drop height.	33
Figure 28.	Impact force comparison showing impact force magnitudes becoming similar again due to damage sustained in both samples for drop height of 71.12 cm (28 in).....	34
Figure 29.	Strain along x-direction at strain gage 1.	35
Figure 30.	Strain along y-direction at strain gage 1.	35
Figure 31.	Strain along x-direction at strain gage 2.	36
Figure 32.	Strain along y-direction at strain gage 2.	36
Figure 33.	Strain along x-direction at strain gage 3.	37
Figure 34.	Strain along y-direction at strain gage 3.	37
Figure 35.	Strain along x-direction at strain gage 4.	38

Figure 36.	Strain along y-direction at strain gage 4.	38
Figure 37.	CNT reinforced impact force plot for 45 cm drop height.	40
Figure 38.	CNT reinforced impact force plot for 60 cm drop height.	40
Figure 39.	CNT reinforced drop height comparison of dry test [5].	41
Figure 40.	CNT reinforced Sample 1 drop height comparison of impact force for submerged test.	42
Figure 41.	CNT reinforced Sample 2 comparison of impact force for submerged data. ..	43
Figure 42.	CNT reinforced Sample 3 comparison of impact force for submerged data. ..	44
Figure 43.	Non-reinforced drop height comparison of impact force for dry test.	45
Figure 44.	Non-reinforced Sample 1 comparison of impact force for submerged test.	46
Figure 45.	Non-reinforced Sample 2 comparison of impact force for submerged test.	47
Figure 46.	Non-reinforced Sample 3 comparison of impact force for submerged test.	47
Figure 47.	Strain results from dry testing of CNT reinforced joint [5].	48
Figure 48.	Strain data for submerged CNT reinforced Sample 2.	49
Figure 49.	Strain data for submerged CNT reinforced Sample 3.	49
Figure 50.	Strain results from dry testing non-reinforced joint [5].	51
Figure 51.	Strain data for submerged non-reinforced Sample 1.	51
Figure 52.	Strain data for submerged non-reinforced Sample 2.	52
Figure 53.	Strain data for submerged non-reinforced Sample 3.	52

LIST OF TABLES

Table 1.	Strength properties for clear casting of vinyl ester resin [9].....	6
Table 2.	Typical Gel Times using MEKP, DMA, and Cobalt [9].	13
Table 3.	Drop Heights.	21

THIS PAGE INTENTIONALLY LEFT BLANK

LIST OF ACRONYMS AND ABBREVIATIONS

CFRP	Carbon Fiber Reinforced Polymer
CNT	Carbon Nanotube
DMA	N-Dimethylaniline
FSI	Fluid Structure Interaction
MEKP	Methyl Ethyl Ketone Peroxide
MWCNT	Multi-Walled Carbon Nanotube
VARTM	Vacuum-Assisted Resin Transfer Molding

THIS PAGE INTENTIONALLY LEFT BLANK

ACKNOWLEDGMENTS

I would like to express my heartfelt appreciation to the following people who have been vital to my successful completion of this thesis study:

My thesis advisor, Dr. Young Kwon for his mentorship, patience, and guidance throughout the course of my thesis work. His experience, expertise, and vast wealth of knowledge in this area of study were key to my completion of this study.

Tom Christian, for his assistance in the operation and trouble shooting of the test equipment used during this study. His ability to problem solve saved me many hours of frustration. I certainly would not have finished my research without his help.

Most importantly, I would like to thank my beautiful wife Molly for her support and understanding throughout this thesis process. Without her support, none of this would have been achievable.

THIS PAGE INTENTIONALLY LEFT BLANK

I. INTRODUCTION

A. BACKGROUND

1. Composites

Composites are becoming more and more important in today's world. They have been used in the aircraft industry for many years, and are currently attempting to make their way into the maritime industry as well. The application of these composites to the marine military environment is very appealing because of the high corrosion resistance offered by the composite. Another main reason for the use of composite is the very high strength to weight ratio. Similar composites have already made their way into the military marine environment. The Navy's DDG-1000 Zumwalt class destroyer has a superstructure made almost completely of composite materials. The use of composites on naval ships is gaining ground because they allow for lighter, faster, and corrosion free ships [1]. Other marine military applications include the use of composites to build ship's rudders. Composite rudders can be shaped and built from a mold, which allows for a much lower cost than a steel rudder of the same design, while having similar strength properties [2]. It has been estimated that the cost of corrosion and corrosion related maintenance cost the U.S. Navy approximately \$22 billion annually [3]. The downside to using composite materials for ship building and shipboard applications is the cost of construction and the cost of training for construction. It is estimated that ships made of composites can cost up to 20% more than a ship made of steel. Other than the superstructure, the navy has looked into composite application to rudders, propellers, stairwells, handrails, valves, and armors [4].

2. Fluid Structure Interaction

Fluid Structure Interaction (FSI) is very important in the application of composites to the marine environment. There is no FSI issue with using composites on parts of the ship that are above the water line because they perform as expected for their given application. However, a problem does arise when the composite is used in a place where a fluid such as water can interact with the composite. It is known that composites

have similar strengths to that of steel. This is the reason why the Navy decided to use a composite for the sonar dome of the DDG-1000. The FSI side of this application was not properly studied, and it resulted in a failure of the composite sonar dome. The reason it failed is due to the fact that composites have a density similar to that of water, as opposed to steel which has a much greater density than that of water. The similar densities play a larger role in FSI. The low velocity impact in water can be very critical to the transient dynamic response of the composite. The added mass effect of the water causes a large amount of stress and strain on the composite that it would not encounter in air. This causes the composite to fail in water more rapidly. This problem does not occur in steel because there is much less of an added mass effect of the water because the density of steel is so large compared to water.

B. OBJECTIVES

The objective of this study is to continue work of previous thesis students and further the study of FSI and its effects on composite materials. In the research conducted by Violette [6], FSI was studied under three different testing conditions. The first condition was a dry impact in air. The second and third cases had impacts while submerged in water. Both cases had the top surfaces of test plates, where impacted, in contact with water, but the bottom surfaces were different. The second case had also a wet bottom surface, called water-backed, while the third case had a dry bottom surface, called air-backed. Those loading conditions represented impact on the ship hulls from the water side. This study will continue that research for different loading condition such that the impact side is dry while the opposite side is wet. This is done to simulate an impact from the inside of a composite hull.

The second part of the research continues the work conducted by Tan [5] on the CFRP coupons, with both non-reinforced, and Carbon Nanotube (CNT) reinforced joint interfaces.

The study of the strength in composite joint interfaces is very important. It is not always possible or practical to build a composite structure in one solid piece. There are many times when a structure must be built from a number of smaller composite sections.

There have been studies aimed at identifying the benefits of CNT joint reinforcement in composites. It was found by Faulkner and Kwon [7] that strength and fracture toughness in CFRP joints is improved through CNT reinforcement. However, this testing was done under static loading.

Data has already been collected for the dry-air only environment. This study will finish the research by conducting the submerged water-backed testing and analysis. The purpose of this part of the study is to continue the investigation of the influence of CNT reinforcement on the behavior of CFRP joint interfaces under low velocity impact loading in a dynamic environment along with FSI.

THIS PAGE INTENTIONALLY LEFT BLANK

II. EXPERIMENTAL METHODS FOR E-GLASS COMPOSITE

A. MATERIALS

There are two main materials used to form the composite and there are many other materials used as tools to accomplish the production. The two most important materials for the composite composition are the resin and the E-Glass woven fabrics. This section talks about the material properties of the resin and the E-glass woven fabrics, as well as the other materials required to complete the process and how they are used.

1. E-Glass

The composite was made using a woven fiberglass cloth known as a 6 ounce E-Glass. These types of woven fiberglass cloths are very common for marine composite construction and repair. The E-glass composite was purchased from US Composites. US Composites offers a variety of different fiberglass cloths, but the woven cloth was chosen for its uniformity and because of the fact that it is lightweight and is very common in small boat building. If this E-Glass is paired with the correct resin it can maintain a high corrosion resistance and provide a water proof layer [8].

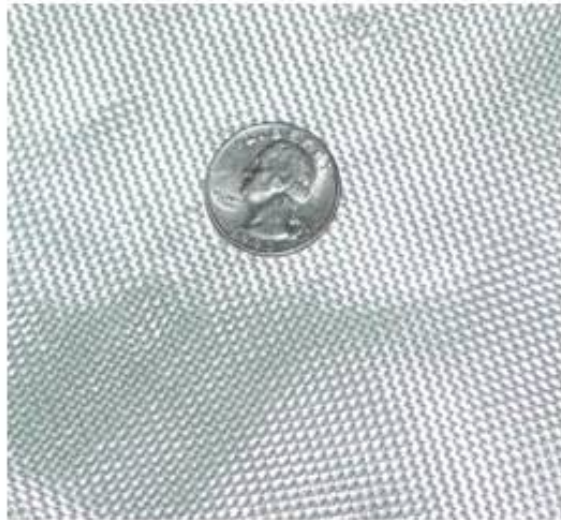


Figure 1. Six ounce E-Glass weave.

2. Vinyl Ester Resin

The resin chosen for this composite fabrication was a Vinyl Ester Resin known as Derakane 510A. As stated above, a smart choice of resin could improve the qualities of a composite material. This particular resin improves corrosion resistance and also has certain fire retardant properties which make it perfect for shipboard use as well as other marine applications. The method used for hardening of the resin is known as clear casting. Clear casting is accomplished by allowing the resin to cure at room temperature for 24 hours and then another 2 hours at a temperature of 120 degrees Celsius, or 25 degrees Fahrenheit. The strength properties of the resin for clear casting are shown in Table 1 [9].

Table 1. Strength properties for clear casting of vinyl ester resin [9].

Property of Clear Casting at 25°C (75°F)	Value (SI)	Value (US)
Tensile Strength	86 MPa	12,300 psi
Tensile Modulus	3400 MPa	490 kpsi
Flexural Strength	150 MPa	21,700 psi
Flexural Modulus	3600 MPa	520 kpsi

3. Hardening Agents for Resin

There are three main hardening agents used for the fabrication process of the composite sample. Two of them are always required and the third is only required if a faster cure time is desired. The first hardening agent is the Methyl Ethyl Ketone Peroxide (MEKP). The second is Cobalt Naphthenate 6%, and the third is Dimethylaniline (DMA).

a. Methyl Ethyl Ketone Peroxide

MEKP, shown in Figure 2, is a basic catalyst which is usually added to polyester and vinyl resins. The addition of the MEKP causes a chemical reaction and heat generation which begins the hardening process in the resin.



Figure 2. Methyl Ethyl Ketone Peroxide (MEKP).

b. Cobalt Naphthenate

The second hardening agent, shown in Figure 3, is a deep blue purple liquid known as Cobalt Naphthenate 6%. Since this is a cobalt solution, its main role in the process is as an oil drying agent, but it also adds some waterproofing to the composite material as well. It is used as a crosslinking catalyst during the hardening process of the fabrication and this particular catalyst is an oxidation dryer with the strongest drying activity. The Napthlenic acid is added to make the cobalt more oil soluble.

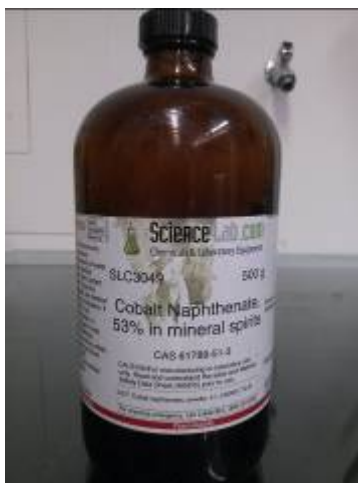


Figure 3. Bottle of Cobalt.

c. Dimethylaniline

Dimethylaniline, shown in Figure 4, is the third hardening agent used in the process. The DMA serves as a promoter to the curing of the resin during the fabrication of the composite. This hardening agent is used for a more rapid curing process of the resin and is only used when fast curing times are desired.



Figure 4. Bottle of Dimethylaniline (DMA).

B. COMPOSITE CONSTRUCTION METHOD

1. Vacuum Assisted Resin Transfer Molding

The process used to fabricate the composite samples used in this research is known as vacuum assisted resin transfer molding (VARTM). VARTM is a very common method used in low pressure composite molding production. This is done by constructing an air tight vacuum around the materials used to make the composite. A vacuum pump is used to expel all the air from the preform assembly of the composite. Once there is an air tight seal, the resin is pulled through the preform of e-glass weave from the bottom to the top. A distribution medium is used to accelerate the processing time of the VARTM and it also ensures total coverage of the preform [10].

2. Materials

There are many different materials needed to complete the VARTM process. A list of all the materials used is shown below.

- E-Glass
- Vinyl Ester Resin
- Airtech Resinflow 75 Distribution Medium
- Teflon
- Peel Ply
- Stretchlon 200 1.5 Vacuum Bag Film
- AT-200Y Sealant Tape
- Plastic Tubing
- Resin Trap

The distribution medium is a green mesh fabric that is used to evenly distribute the resin throughout the whole preform. The Teflon is used to prevent the resin from adhering to the glass, which is used at the base of the set up. Peel ply is a nylon material that is placed between the distribution media and the e-glass weave for easy release after curing. The vacuum bag is made from a Polyolefin material and is used to cover the preform and adhere to the sealant tape to achieve a vacuum around the preform. The sealant tape is to hold down the vacuum bag. The plastic tubing is used to transfer the resin through the preform from the resin reservoir to the resin trap. Finally, the resin trap is used to collect any waste resin during the VARTM process.

3. Procedure

a. Preparation and Layup

The entire preform is put together on a glass foundation. It is important to ensure that the glass foundation is clean and free of any previously cured resin so that it does not contribute to any deformation of the next composite. The finished preform layup will take the form shown in Figure 5.

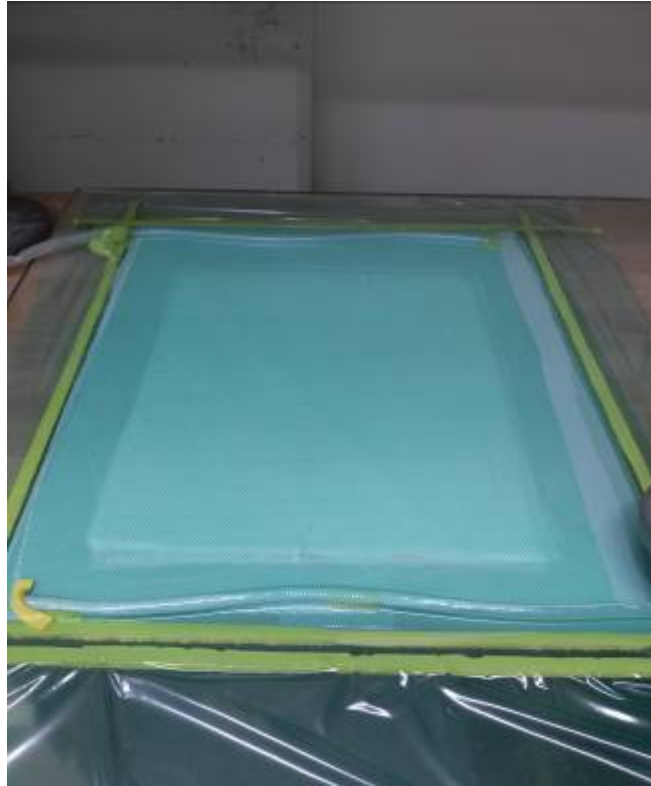


Figure 5. Final product of preform layup.

The first step in the process is to cut all required materials for the layup. Once the size of the composite sample is determined, the cutting of the material can begin. The over size is not too important and does not need to be exact. Cut 14 sheets of E-Glass material to the desired size of the sample, in this case the size of the composite sample was approximately 38.10 cm (15 in) by 45.72 cm (18 in). Next, cut 2 sheets of both the peel ply and the distribution media. The distribution media should be cut to the same width as the composite, 38.10 cm (15 in), but the length should be cut approximately 5.08 cm (2 in) longer. This helps to ensure a complete distribution of the resin during the transfer.

The peel ply should be cut the same width as the composite, 38.10 cm (15 in), but it must be a few inches longer, similar to the distribution media. The purpose of the peel ply is to aid in easily removing all the fabrication materials from the finished composite. The extra few inches allow for a place to grab when it is time to remove all the material.

The next step is to determine the size of the preform so that the sealant tape and vacuum bag may be put in place. The easiest way to go about this is to place the peel ply down first and make a box around it on the glass with the sealant tape. Since the peel ply is the largest piece in the preform we know it will not need to be any larger. Once the sealant tape is laid out, place the Teflon down over the glass as a boundary which will help in safely removing the composite from the glass base.

Now it is time to start placing the materials down over the Teflon. The order in which the materials are laid out is important and it should follow Figure 6 taken from McCrillis [11].

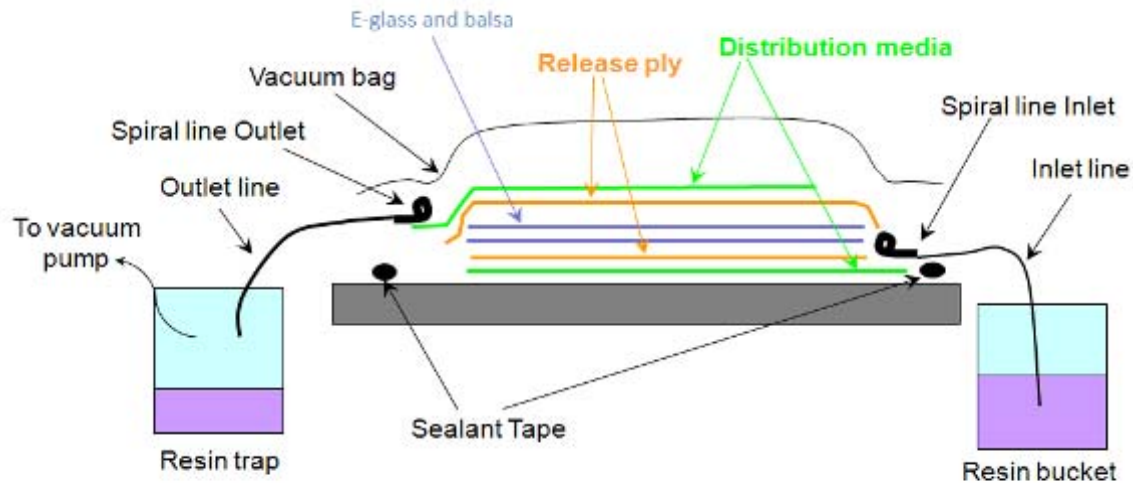


Figure 6. Preform Layup [11].

Once the materials are placed onto the glass foundation the next step is to begin the routing of the plastic tubing. There is no one correct way to accomplish this task, but the method used in this research seemed to be the most convenient. The first tube, which will be used to pull the resin into the preform, should be long enough to reach the resin bucket at one end while the other end is placed over the sealant tape to hold it in place. The objective here is to have the resin pulled in at the very bottom of the composite sample because the second plastic tube is placed at the other end of the composite in the exact same manner and is connected to the resin trap. Sometimes it

helps to add more sealant tape and/or place small weights over some of the tubing to help keep it in place. In the past, other students have used very rigid plastic tubing that can be difficult to keep in place. A clear and much more malleable plastic tubing was used in this research instead and was found to be much more practical. The two plastic tubes are compared in Figure 7.



Figure 7. Comparing the flexible tubing to the stiff tubing.

b. Resin Preparation

The resin preparation is the most important part of the process. An incorrect mixture of resin and hardening agents will make the difference between a good sample and one that is not usable. The first step to the resin preparation is to pour the desired amount of resin into your resin bucket. For the composite samples made for this research, one liter of the resin was sufficient for the process. Once the desired amount of resin is in the bucket, it is important to measure out the exact amounts of hardening agents needed for the desired curing time. Table 2 shows the amount of each hardening agent needed for the desired cure time at the current room temperature. The values given are in parts per hundred resin molding compound (phr).

Table 2. Typical Gel Times using MEKP, DMA, and Cobalt [9].

Gel Times at 25°C (75°F)	MEKP (phr)	Cobalt (phr)	DMA (phr)
15 +/- 5 minutes	2.00	0.30	0.05
30 +/- 10 minutes	1.25	0.30	-
50 +/- 15 minutes	1.00	0.20	-

It is important to note that the gel times of this mixture will vary based on the surrounding environment. This is why it is so difficult and important to come up with a mixture that works well and stick to that mixture. The gel times for approximately 50 minutes was used in this research. Also, 1 drop of DMA from a 3mL syringe was used as well. It was found that using a 30 minute gel time mixture made it difficult for the resin transfer process to completely cover the preform. When using the 50 minute gel time, sometimes the resin was unable to set and the vacuum began to pull resin from the preform after the transfer was stopped. The DMA was added to help the resin set faster into the preform.

Another important part of the mixture process is how to actually mix the components. It was discovered during the first couple trials that the MEKP and Cobalt react to one another if they are added at the same time. To fix this problem, the MEKP was added first and thoroughly stirred into the resin before the Cobalt was added. In addition, once all the required components are added to the resin it is important to keep mixing it on and off for approximately 15 minutes to allow for a proper mixture. Once the air bubbles stop forming in the mixture it is ready to go.

C. POST FABRICATION METHODS AND REQUIREMENTS

1. Curing

The curing process is relatively simple, but it takes some time. After the resin transfer is complete, the tube used on the resin side of the preform is clamped to keep the vacuum seal intact. Now the vacuum must stay on for eight hours during the initial cure period. Then the composite must cure another 24 hours with the vacuum off. Both of these cure processes take place at room temperature. The last step in the cure process is to cure the composite for another six hours at an elevated temperature of 160 degrees F.

2. Sizing

Once the curing is complete the samples will need to be cut down in size. The overall size of the composite must be able to fit into the impact machine, but there is no correct exact size. The only important part of the sizing is the 30.48 cm (12 in) by 30.48 cm (12 in) test area. To keep the test area consistent, a grid of 7.62 cm (3 in) by 7.62 cm (3 in) squares were drawn onto the sample. This allowed for a consistent placement of the strain gages on each composite sample.

3. Strain Gages

The strain gages were an important part of this research. They gave great insight into the mechanics of what is actually occurring during the testing of each sample. They showed a quantitative difference between each of the testing environments which allowed for a better analysis of the results. The strain gage rosette measures the strain in the composite during the testing. The strain is measured in three different directions per strain gage. The measurement of strain in three different directions is very important because they allow us to determine the principal strains and stresses.

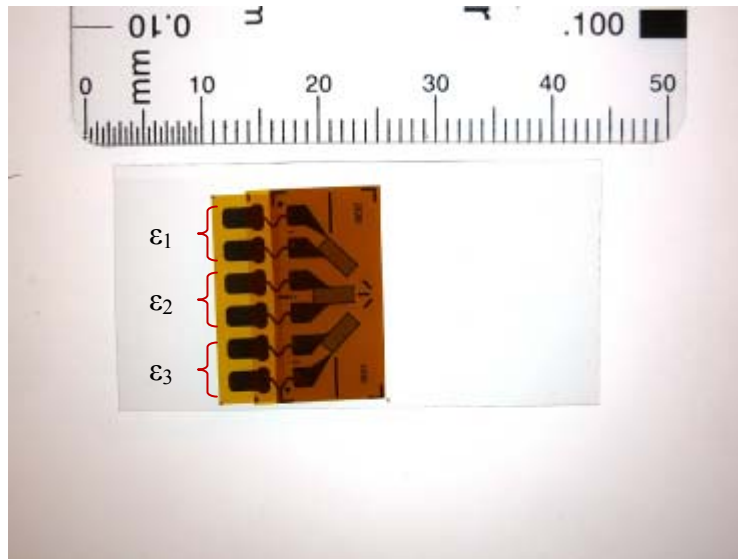


Figure 8. Square strain gage rosette showing ϵ_1 , ϵ_2 , ϵ_3 .

a. Overview

This strain gages used for this research were from Vishay Precision Group. Each square composite sample had four strain gages placed throughout the surface of the sample. Figure 8 shows the strain gage rosette channel configuration. Figure 9 shows the arrangement of strain gages used for the square composites. The CFRP samples each had one strain gage placed at the center of the test area directly under the impact zone. This is shown in Figure 15. All the technical data and required equations for the strain calculations are contained in the Tech Note TN 515 [12]. The layout shown in Figure 9 results in the transformation equations becoming:

$$\epsilon_x = \epsilon_1$$

$$\epsilon_y = \epsilon_1 + \epsilon_3 - \epsilon_2$$

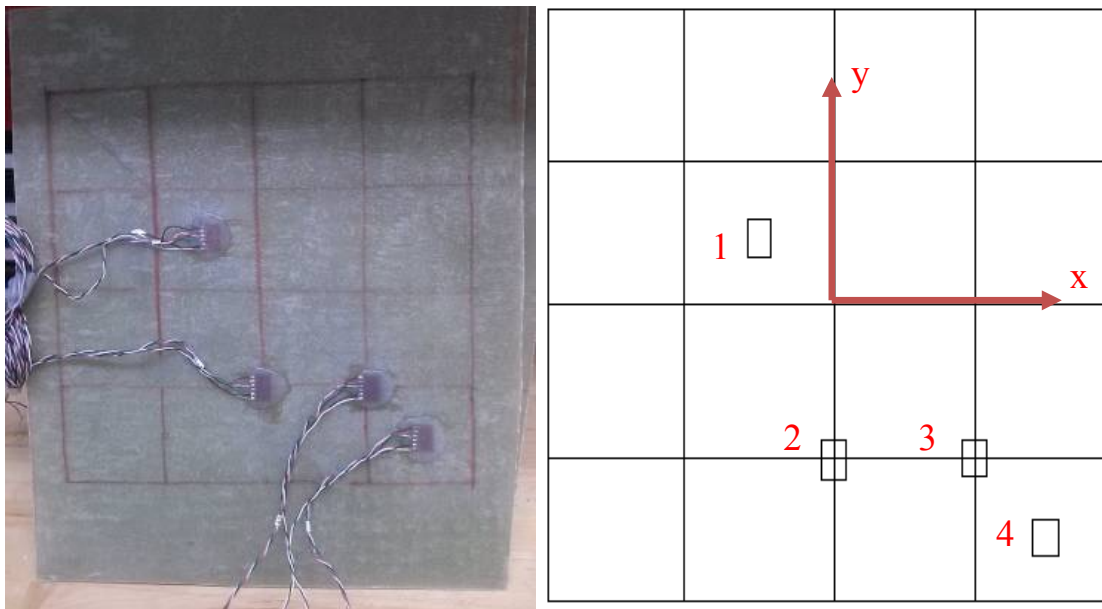


Figure 9. Strain Gage layout on composite samples.

b. Application to Composites

Application of the strain gages is another very important part of the process. There is a very simple method to ensure proper adhesion of the strain gages to

the samples. The first step is to lightly sand the area where the strain gages will be placed. Next, the surface of the material must be cleaned with a surface cleaning agent prior to adhesion. The strain gages were affixed to both composite samples using a M-bond AE-10 shown in Figure 10. This is a two compound, 100% solids epoxy system for general purpose stress analysis. For testing done in water, a water proof coating was placed over the strain gages. This coating is a non-corrosive silicon rubber, RTV. All of the application methods were taken from application notes from the Vishay website [13].



Figure 10. M-bond AE-10 strain gage adhesive [13].

D. TEST EQUIPMENT

The only piece of test equipment used in this research was a drop weight test machine designed by a previous student at NPS [14]. The impact machine was used for testing both composites used in this research. The impact machine is a simple drop weight system that allows the user to drop a desired amount of weight from a desired height. Figure 11 shows the apparatus. The test machine gets lowered into the tank during testing to give the best stability possible. It is also to keep the testing consistent. The water based testing is done in the tank and therefore the air based testing is as well.

The drop weight apparatus has two main components. The first is a trigger that starts the data acquisition process at the same height for each drop. The second

component is at the tip of the impactor itself. The impactor has a built in force sensor and for each drop the force data is acquired using a specifically designed LabVIEW program. The LabVIEW program recorded 1000 samples of data over a 100 millisecond period of time. This was consistent throughout the testing of both composite samples.

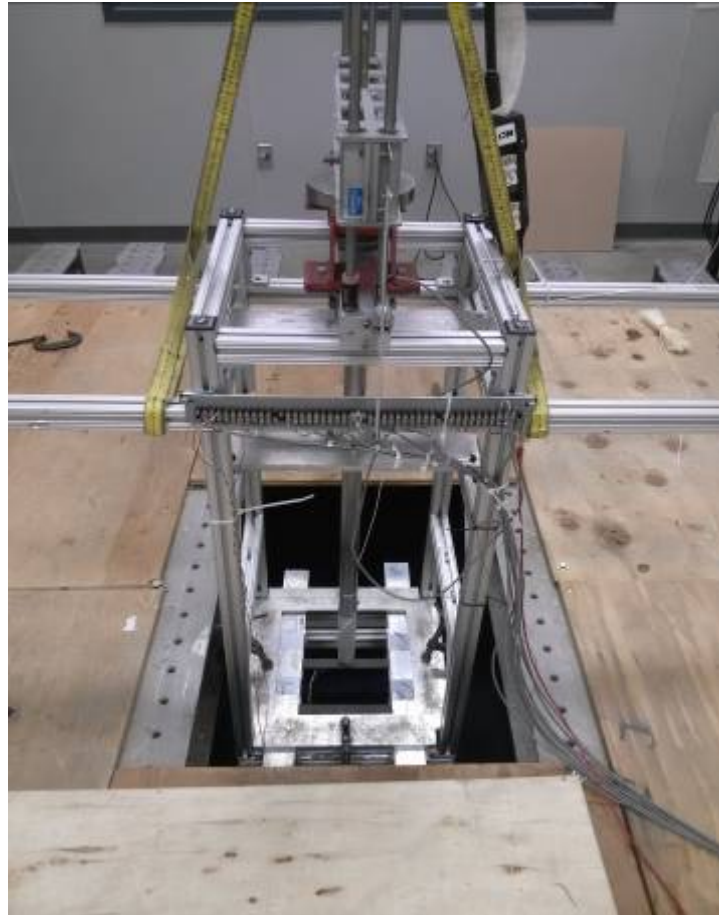


Figure 11. Impact test machine.

E. TEST METHODS

1. E-Glass Composite Sample

A primary goal of this study was to determine the amount of force that initially caused damage to the composite sample. This allowed for the data before and after the damage to be analyzed and compared/contrasted. The damage was attempted to be detected visually after each drop. The initial damage is considered to be at the time the first delamination of the composite is visible. This testing gives great insight into when

damage can be expected to occur and how that damage will affect the composite after more impacts are experienced.

a. Setup

The first test done was the dry impact test. This was done to use as a baseline test so that the differences in damage, force, and strain data could be compared between the two test environments. This test was repeated 3 times to show consistency in the data being obtained and determine its reliability. The results from the dry testing are shown in Chapter III.

The next test was done in the water environment. A Plexiglas box was fabricated to fit over the top of the composite sample in order to keep the top of it dry while being lowered into the water filled tank. The goal of this testing was to determine the FSI with the composite during impact testing with a water backed, dry top test environment throughout a set of different drop heights. The drop heights used were also identical to the heights used in Violette [6]. This environment could be thought of as a simulated patch on a ship, or piece of equipment vibrating on a composite deck. The setup of the test apparatus is shown in Figure 12. It was initially sealed with silicone based sealants. However, these failed after about two drops on the sample and water was able to fill the box.

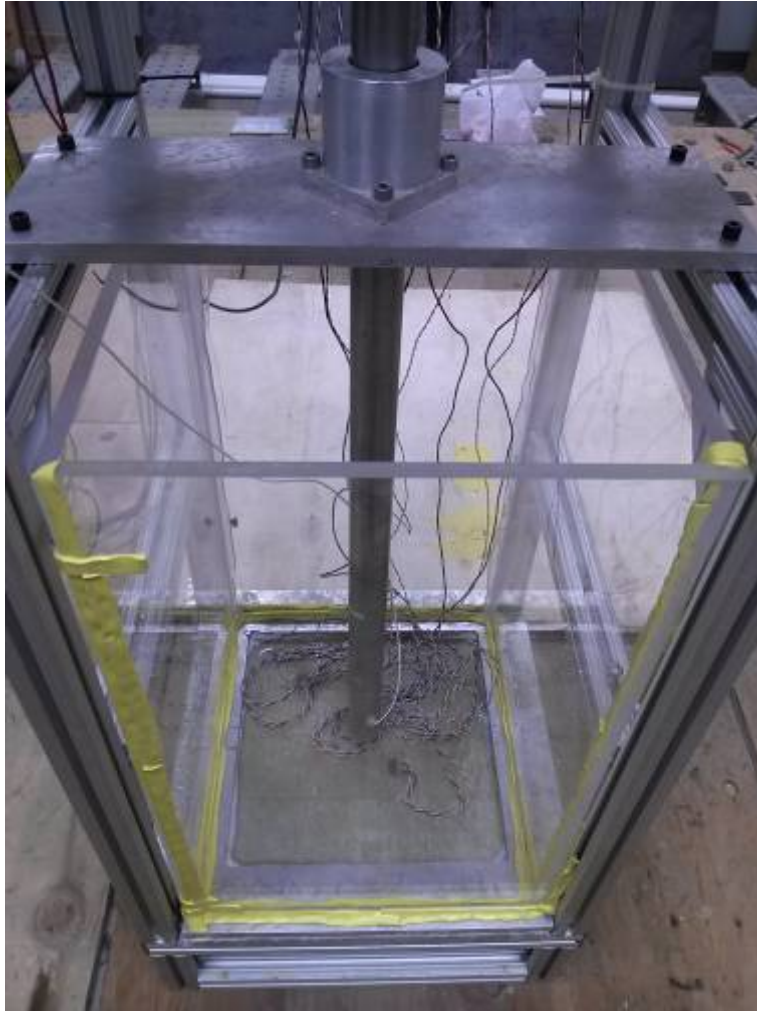


Figure 12. Plexiglas box used to keep the top of the composite dry while being submerged in a water filled tank.

To fix this problem, the box was resealed with the same silicon sealant as a first layer of protection. Then expanding spray foam was used to cover the silicon sealant and any other areas of concern. This solution was able to keep water out of the box for the entire duration of the testing and it is shown in Figure 13.



Figure 13. New setup using expanding spray foam as a second layer of water proofing.

b. Drop Weight and Drop Heights

The test methods used to gather data on the E-glass composite samples were exactly the same as the methods described in the paper by Violette [6]. In that study, three different drop weights were used. For this testing I chose to use the larger weight of 10.8 kg. This weight was chosen because a balsa wood core was used in the previous study. Instead, 16 layers of the E-glass were used to form the composite for the present study, and early initial testing showed little to no visual damage with the lower weight.

The weights were dropped from a starting height of 7.62 cm (3 in) and ended with a drop height of 76.20 cm (30 in). These drop heights were chosen because

we know that from 7.62 cm (3 in) no damage will be incurred and at 76.20 cm (30 in) we are approaching the maximum force recording levels of the impact sensor [6]. All of the drop heights are shown in Table 3.

Table 3. Drop Heights.

Drop Number	Height (in)	Height (cm)
1	3	7.62
2	4	10.16
3	5	12.70
4	6	15.24
5	8	20.32
6	10	25.40
7	12	30.48
8	14	35.56
9	16	40.64
10	18	45.72
11	20	50.80
12	22	55.88
13	24	60.96
14	26	66.04
15	28	71.12
16	30	76.20

2. Carbon Fiber Reinforced Polymer Sample

The CFRP samples were made in a similar fashion as the E-glass composite samples. The difference is that two CFRP samples were joined together during the VARTM process to form a composite joint interface. This interface was then pre cracked with a crack length of 150 mm. There were two different types of the CFRP samples. The first had a simple non-reinforced joint interface. The second had a Carbon Nanotube reinforced joint interface. The CFRP samples were then cut into coupons as shown in Figures 14 through 16. A detailed explanation of the fabrication process and CNTs used can be found in the work done by Tan [5].

The test coupons were placed between two aluminum plates as shown in Figure 15 and then placed into the drop weight apparatus. Then, the coupon was clamped down on all sides to simulate the desired clamped boundary conditions. The strain gages for

this testing were placed directly underneath the impact zone at the center of the coupon. This is shown in Figure 14.

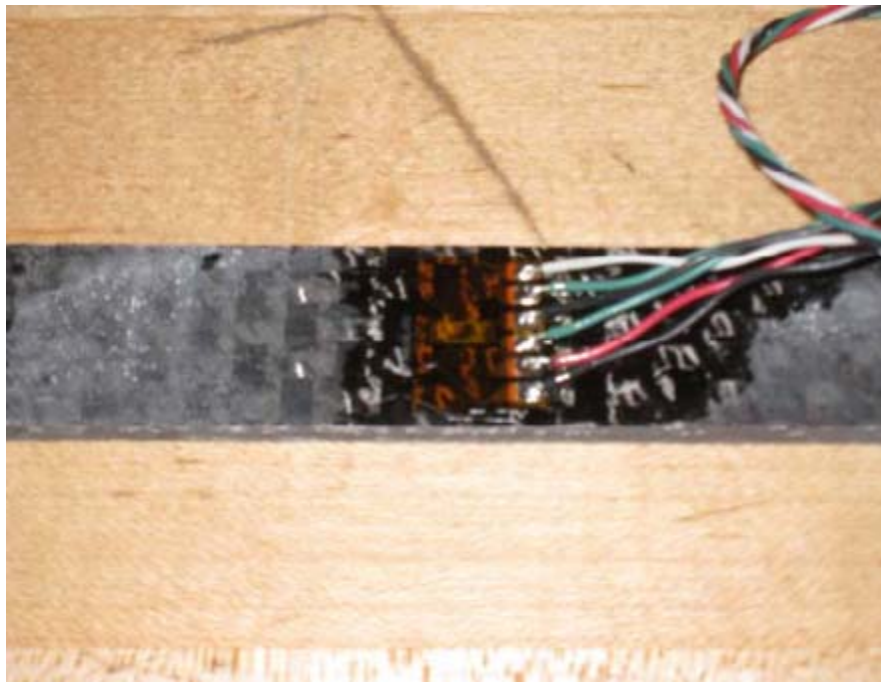


Figure 14. Bonded Strain Gage [5].

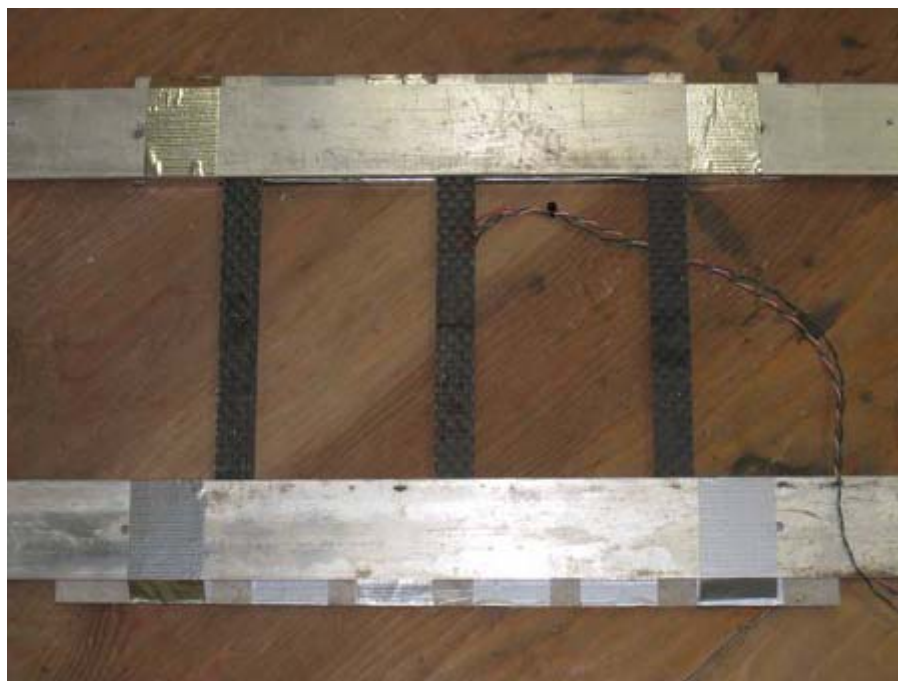


Figure 15. CFRP coupons sandwiched between two aluminum plates [5].

The exact same test conditions were used here as were used by Tan [5], with the exception of the size of the CFRP samples. The overall size was larger, but the same size test area was used. The CFRP coupon size and pre-crack length are shown in Figure 16.

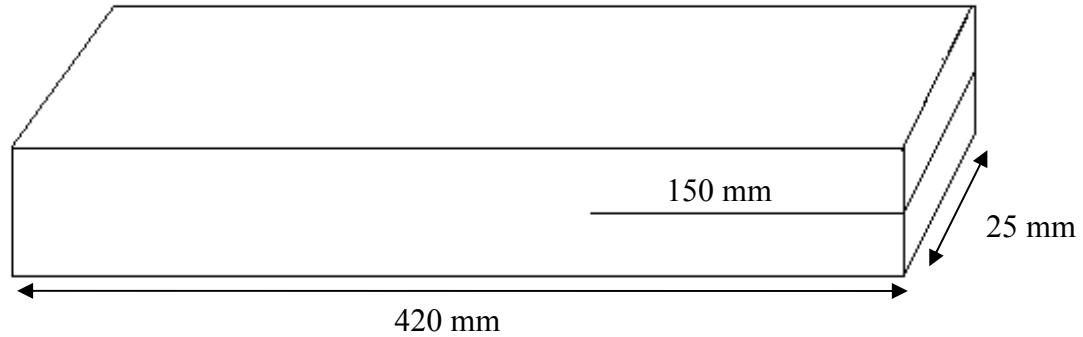


Figure 16. CFRP coupon dimensions.

Once the coupons were secured to the test apparatus, the impact machine was lowered into the tank of water. The actual test consisted of dropping a 2kg weight from varying heights. The drop heights were from 45 cm, 60 cm, 75 cm, 90 cm, and 105 cm. The 2 kg weight was dropped from each height twice. This was done a total of 8 times with 4 CNT reinforced samples being tested and 4 non-reinforced samples being tested. The final test set up with the sample in the water is depicted in Figure 17. The data from the three best results are discussed in Chapter IV.

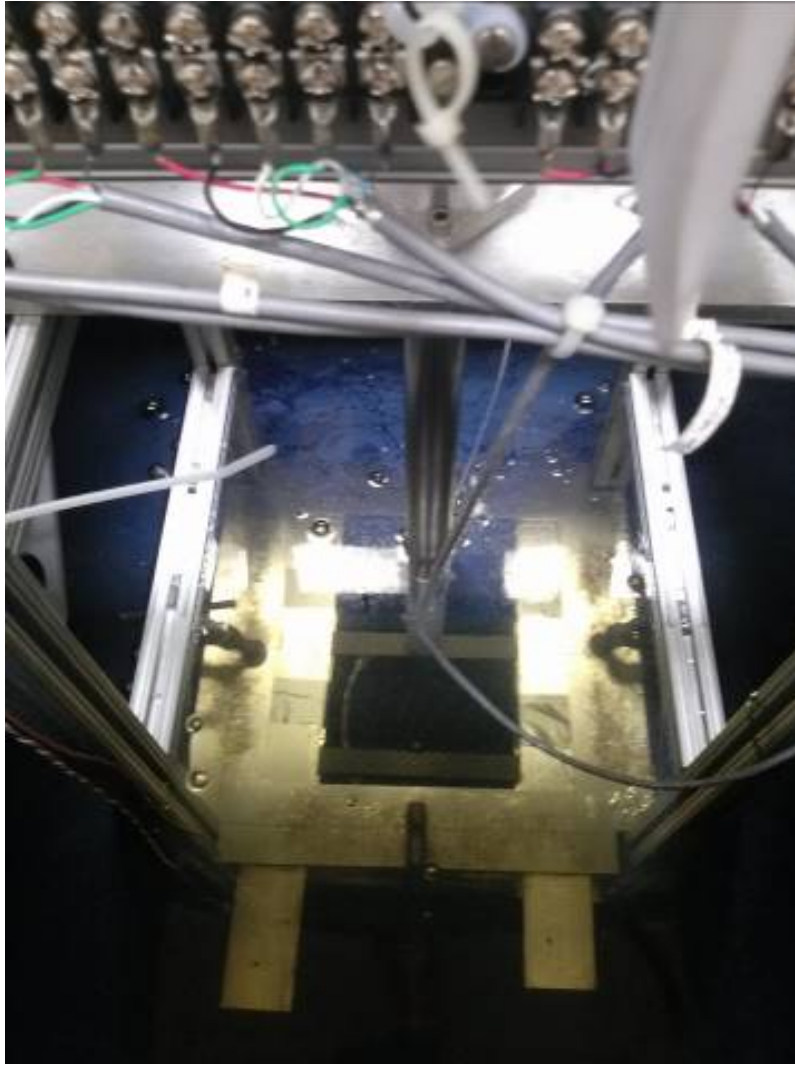


Figure 17. CFRP coupon clamped and ready for water testing.

III. RESULTS AND ANALYSIS

A. E-GLASS COMPOSITE

1. Overview

The goal of this study was to determine the effects FSI has on composite materials and to obtain a better understanding of response of the composites. An important aspect of this study is keeping track of the damage incurred by the composite so that we can determine when the composite fails and how this failure affects the composite's response to further impacts. The damage done to the composites can be hard to detect. Composite materials have distinct modes of failure depending on the type of glass material used to make the composite. In the woven e-glass composites, Delamination of the back side of the composite, where it is in tension after impact, is the most common place for the damage to occur. For this reason, after each impact on the composite sample, the backside was examined for any evidence of damage. All damaged observed during this testing was delamination of the composites. Delamination is one of the most frequent modes of failure in composite materials. Small areas of delamination are capable of reducing the compression strength of composite materials by 50 percent. The most common causes of delamination are tensile and compressive fatigue loading and impact loading [15]. In recent literature there are many great reviews of published papers on the failure modes, and damage identification and significance which can be used as general references [16-19].

For all the samples tested a spreadsheet was used to track the visible damage, or delamination, to the samples. Delamination occurred at a significantly lower drop height during the submerged testing versus the dry testing. Figures 18 and 19 show examples of the delamination occurring at the underside of the impact zone. The overall size of the delamination sites for both dry and wet testing was similar at the end of the testing.



Figure 18. Delamination under impact zone of wet sample.

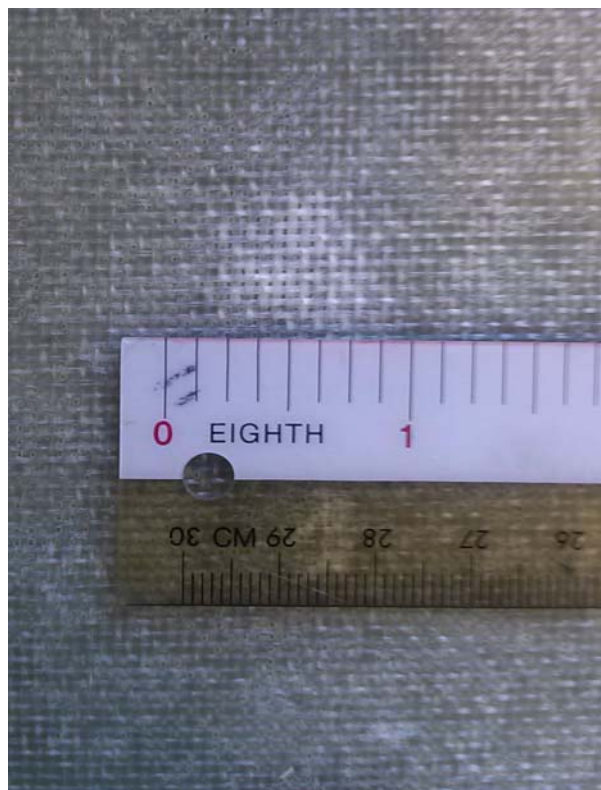


Figure 19. Close up of delamination under impact zone of wet sample.

2. Force Analysis

After only a total of six tests, three in water and three in air, the data proved to be extremely consistent. Figures 20 through 23 show the consistency of the data for two of the samples tested.

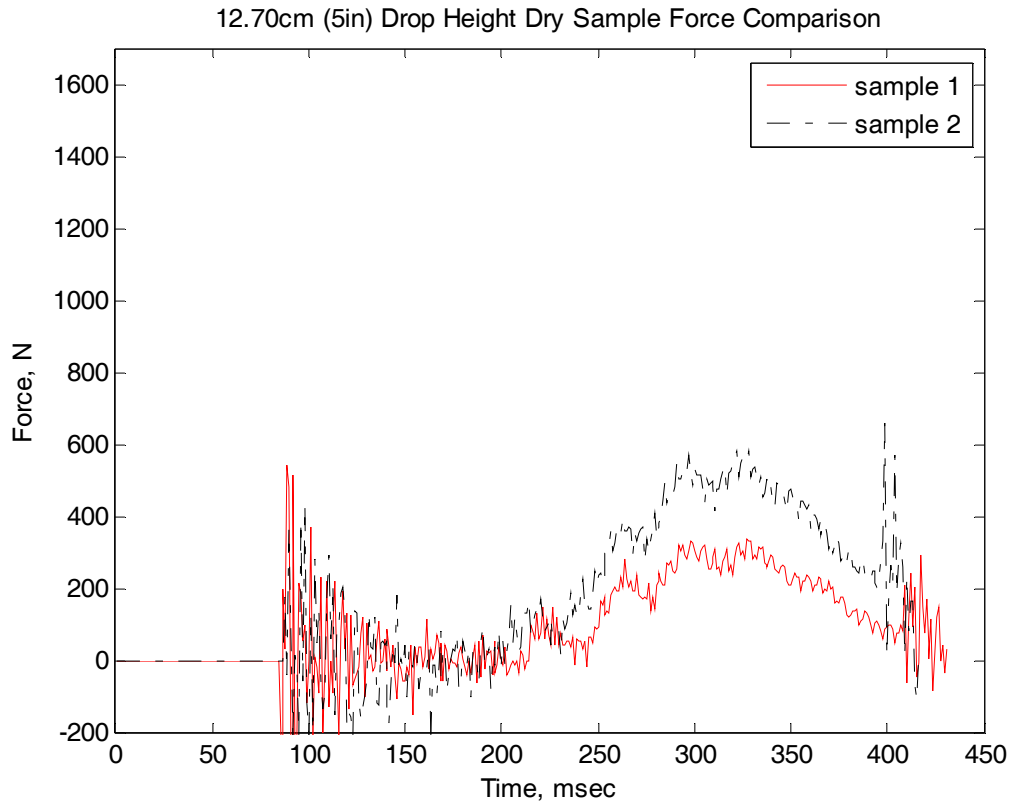


Figure 20. Force comparison of 12.70 cm (5in) drop height dry testing.

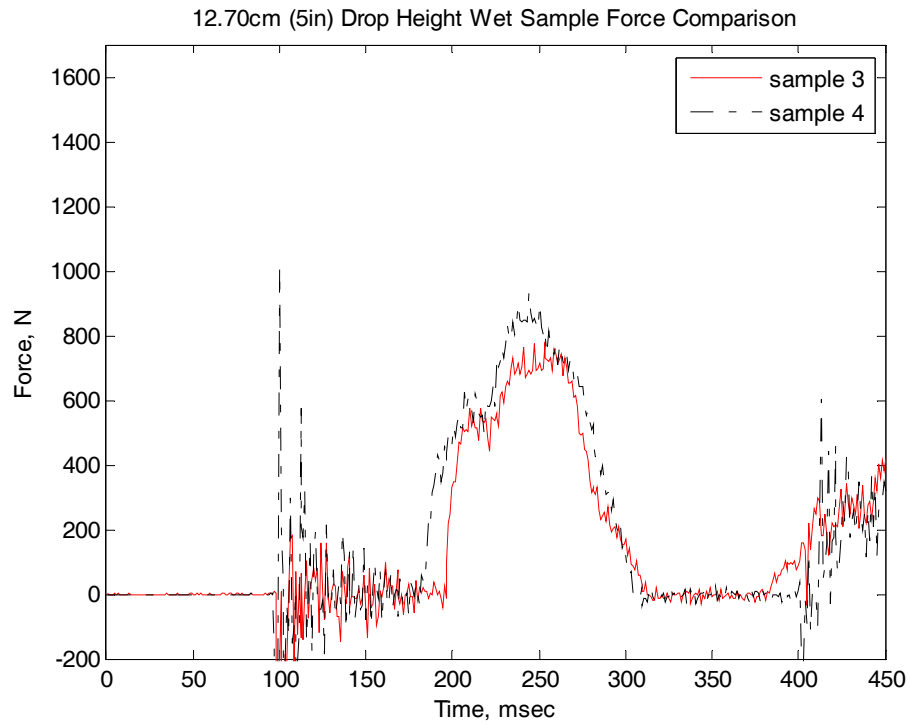


Figure 21. Force comparison of 12.70 cm (5in) drop height for wet testing.

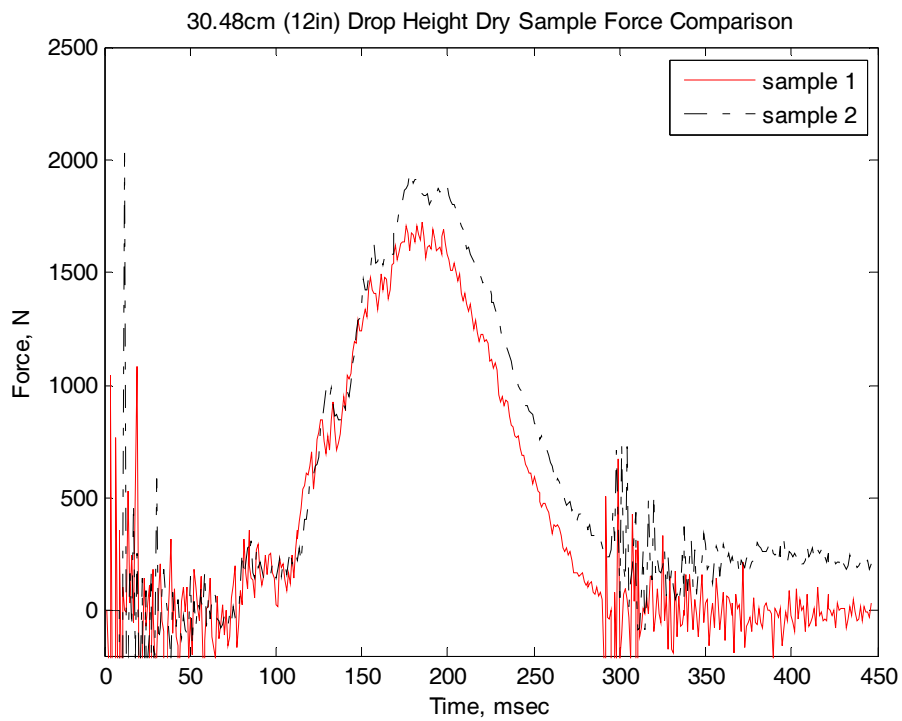


Figure 22. Force comparison of 30.48 cm (12in) drop height dry testing.

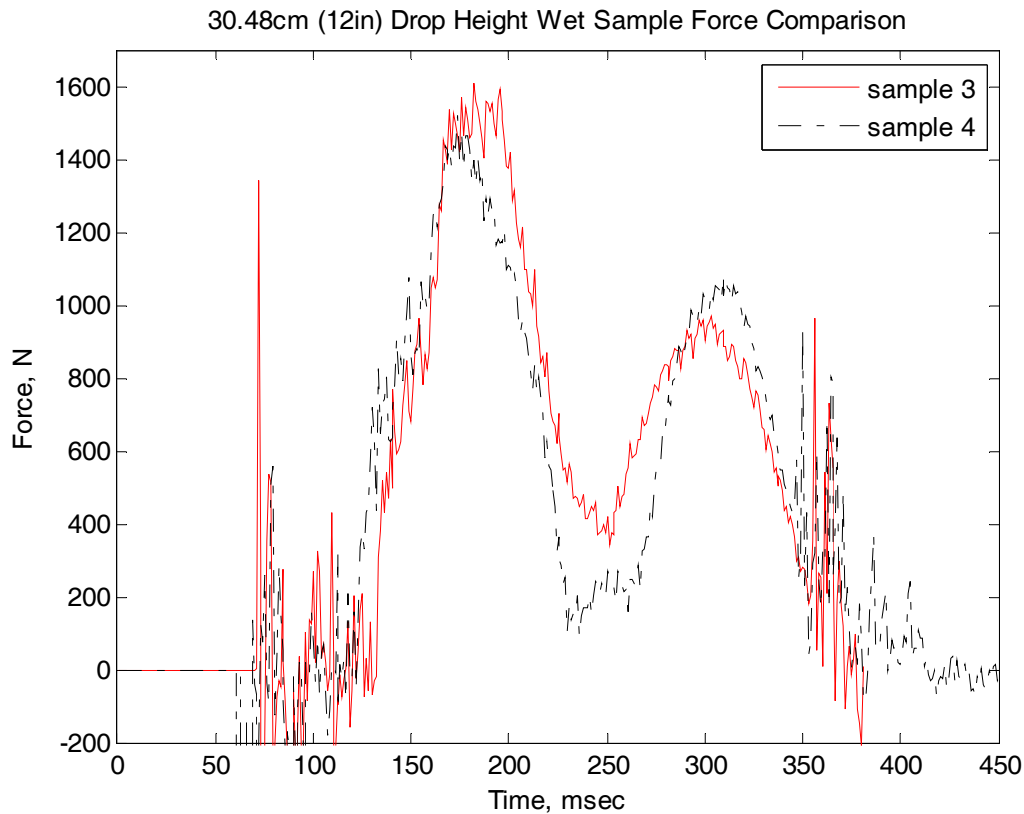


Figure 23. Force comparison of 30.48 cm (12in) drop height for wet testing.

There is plenty of information available from the force data that is collected during the testing. First, we know from previous testing that the impact forces experience in a fully submerged environment is higher than the force in a dry environment for the same drop height. The same was found for the variation of the submerged testing done here. Figure 24 shows that the impact force for a 15.24 cm (6 in) drop height has approximately a 350 N higher impact force than the dry impact. This is exactly what we expect to see. It is important to note that at this drop height, the first sign of delamination occurred at the underside of the sample.

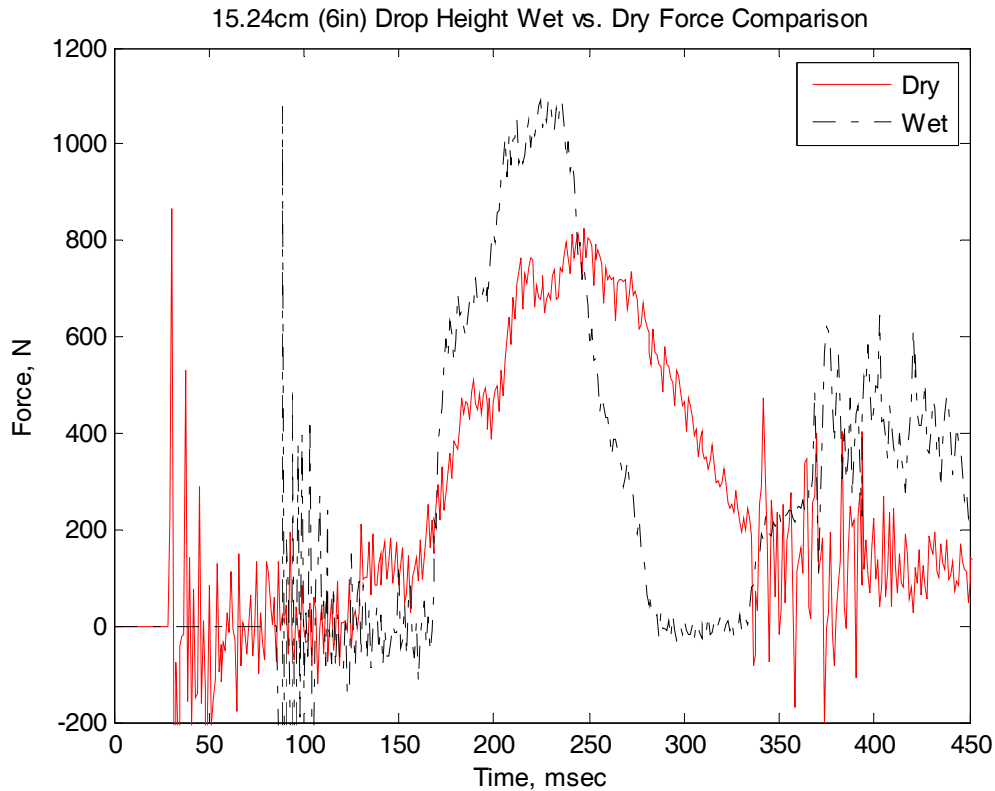


Figure 24. Impact force comparison between wet and dry testing with drop height of 15.24 cm (6 in).

The fact that this drop height is the first sign of delamination is significant because at this point, the impact force for the wet samples will no longer be greater than the dry impact force. As the drop heights increase the dry impact force becomes greater than the wet impact force. In every case, the damage occurred earlier in the wet sample versus the dry sample. In all cases for the wet impact test, a drop height of 15.24 cm resulted in initial damages. However, in all cases for the dry impact test, initial damages occurred between drop heights of 55.88 cm and 71.12 cm. This fact that the change in impact force occurs after damage is significant because even if no visible damage is detectable, the force data can be analyzed to determine if any internal damage has occurred to the composite sample. Figure 25 shows the damage as a function of drop height for both the wet and dry samples.

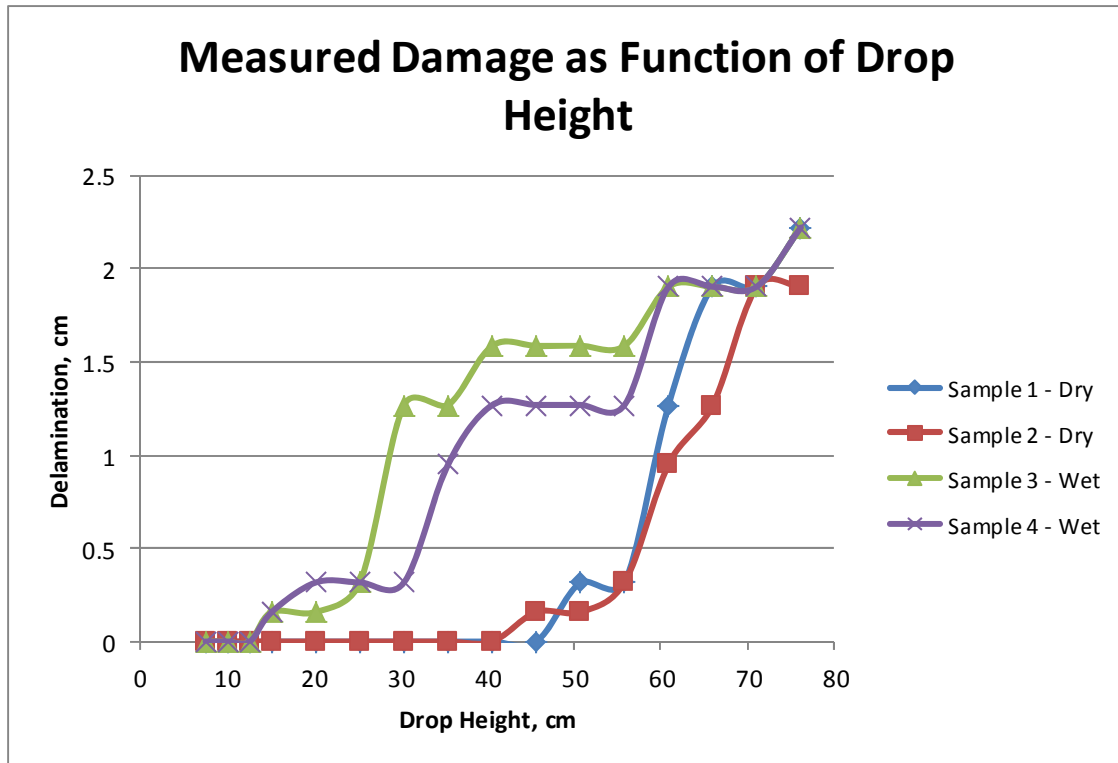


Figure 25. Damage as a function of drop height for both wet and dry samples.

Figure 26 shows how immediately after damage is sustained in the wet sample, the impact force magnitudes are identical. The damaged sample experiences a loss of stiffness and therefore the impact force decreases.

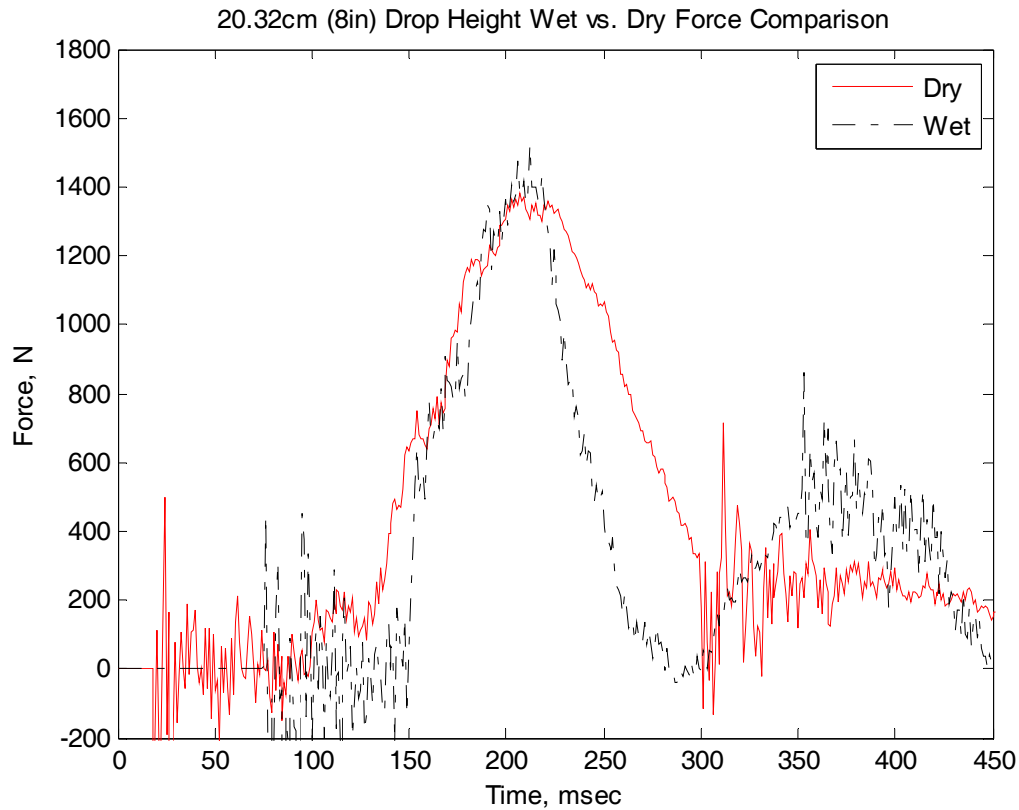


Figure 26. Impact force comparison showing same impact force due to damage in wet sample with a drop height of 20.32 cm (8 in).

Since these low drop heights have caused damage in the wet samples and not yet in the dry sample, the impact force for the dry samples will become larger than the wet samples until damage is incurred. Figure 27 shows how the dry impact force is now much larger than the wet impact force because the dry still has not incurred any damage.

During the testing of the dry samples, visual damage was not noticed until about the 66.04 cm drop heights. So if we look at the wet vs. dry comparison at that drop height we should expect to see the impact forces to be similar again because they have both sustained damage. Figure 28 shows the comparison at a drop height of 71.12 cm and the results are what we expect to see.

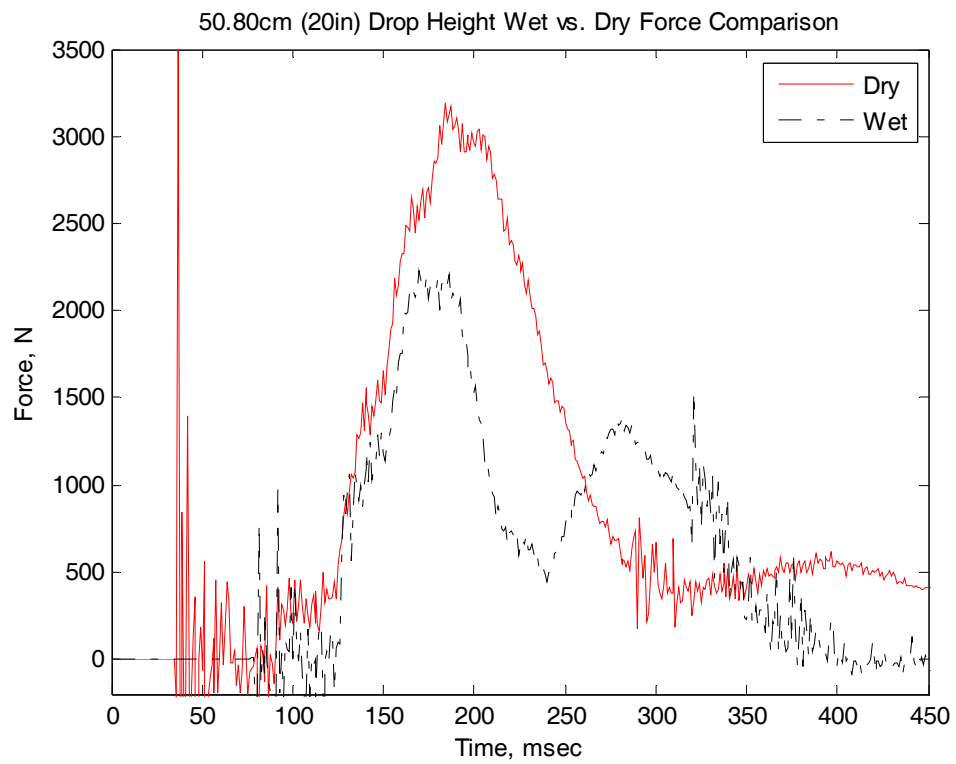


Figure 27. Impact force comparison showing the dry force still larger than the wet force, but smaller difference at 50.80 cm (20 in) drop height.

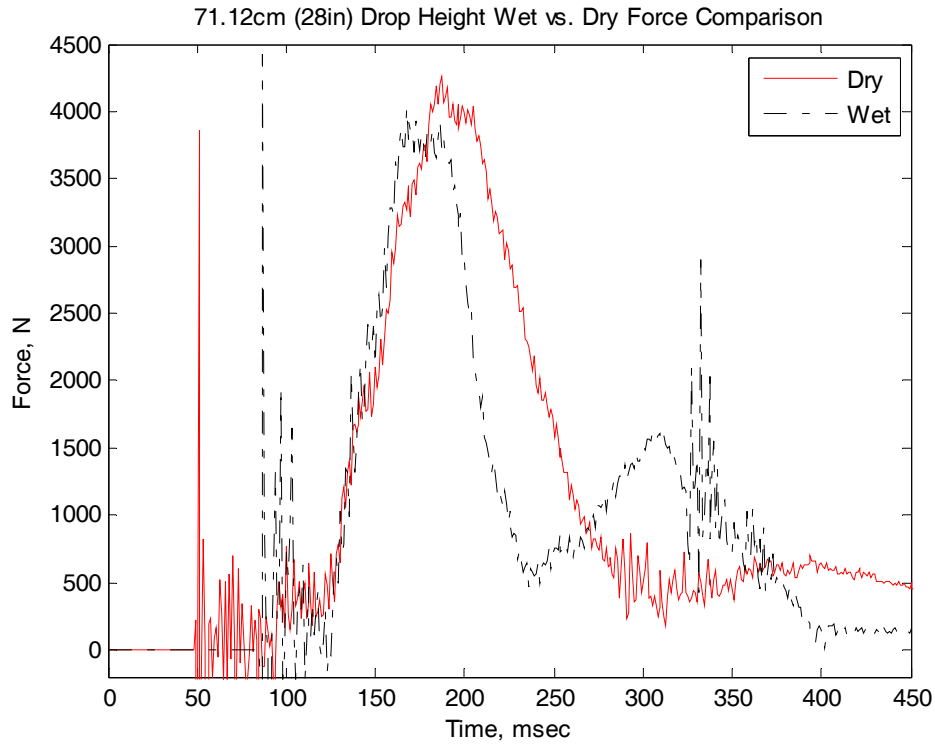


Figure 28. Impact force comparison showing impact force magnitudes becoming similar again due to damage sustained in both samples for drop height of 71.12 cm (28 in).

3. Strain Analysis

The strain data gathered can help determine what is occurring locally in each sample and it gives a great insight into the fluid structure interaction occurring at each impact height. Being able to compare the dry versus wet strain data at the exact same drop height and weight combination is very important in determining how the fluid structure interaction deforms each sample. It is expected that the deformation in the wet samples would be higher at each strain gage throughout the sample than that of its dry counterpart. Strain data for the x and y directions was recorded at the four different strain gages on each sample.

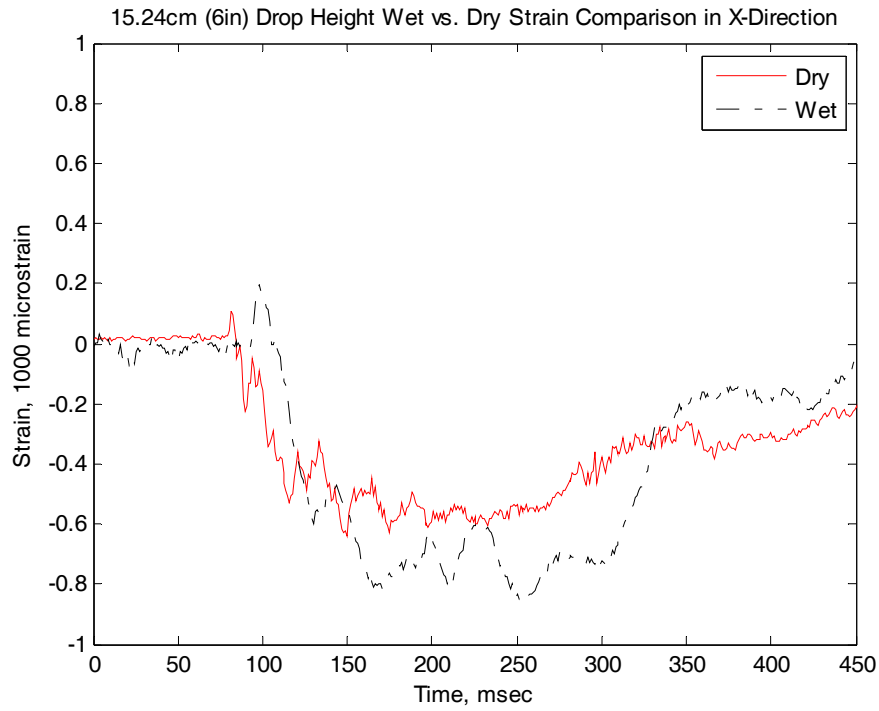


Figure 29. Strain along x-direction at strain gage 1.

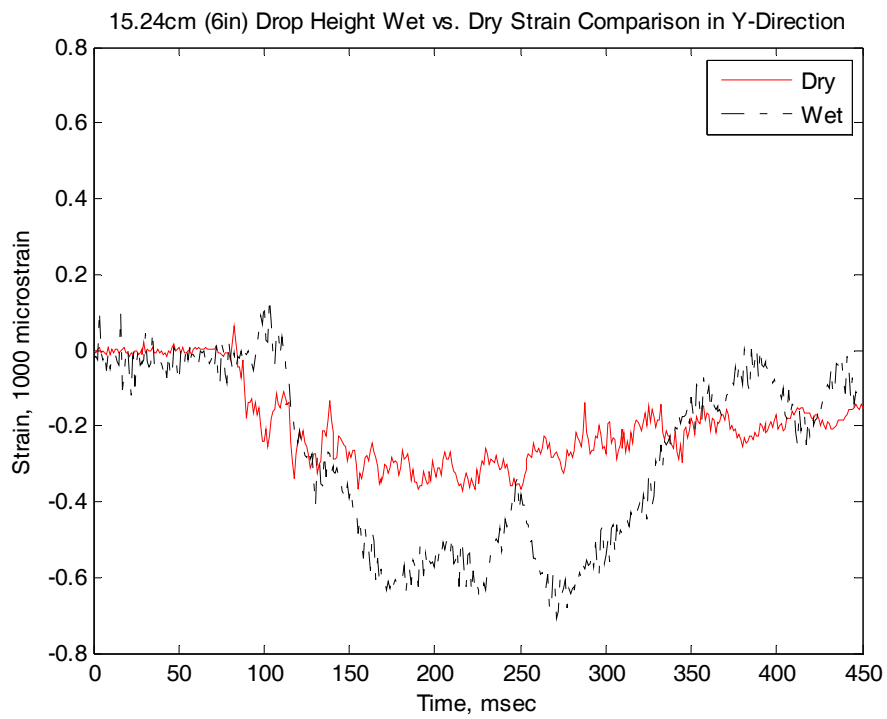


Figure 30. Strain along y-direction at strain gage 1.

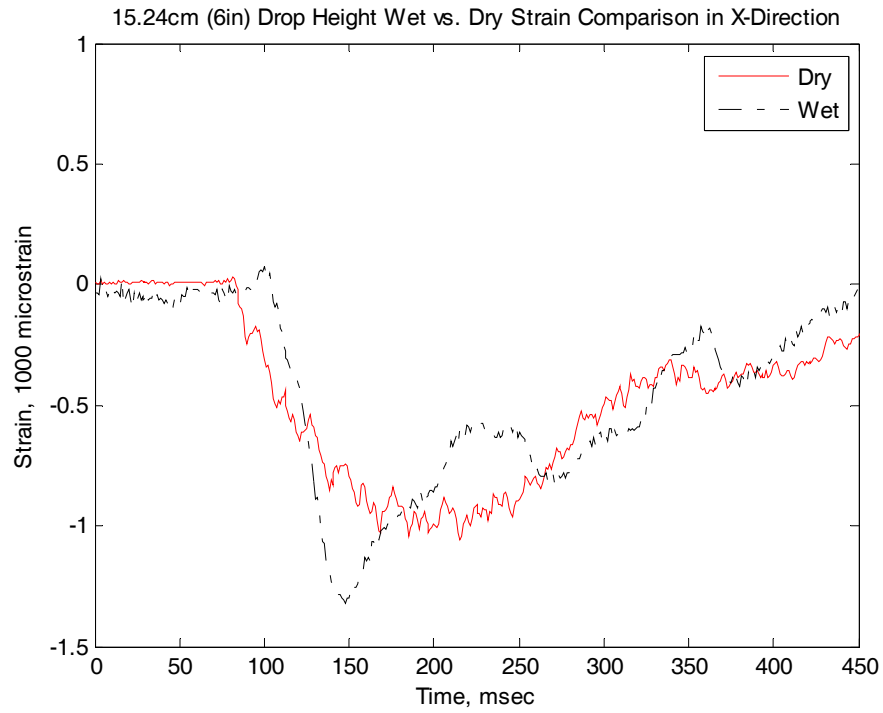


Figure 31. Strain along x-direction at strain gage 2.

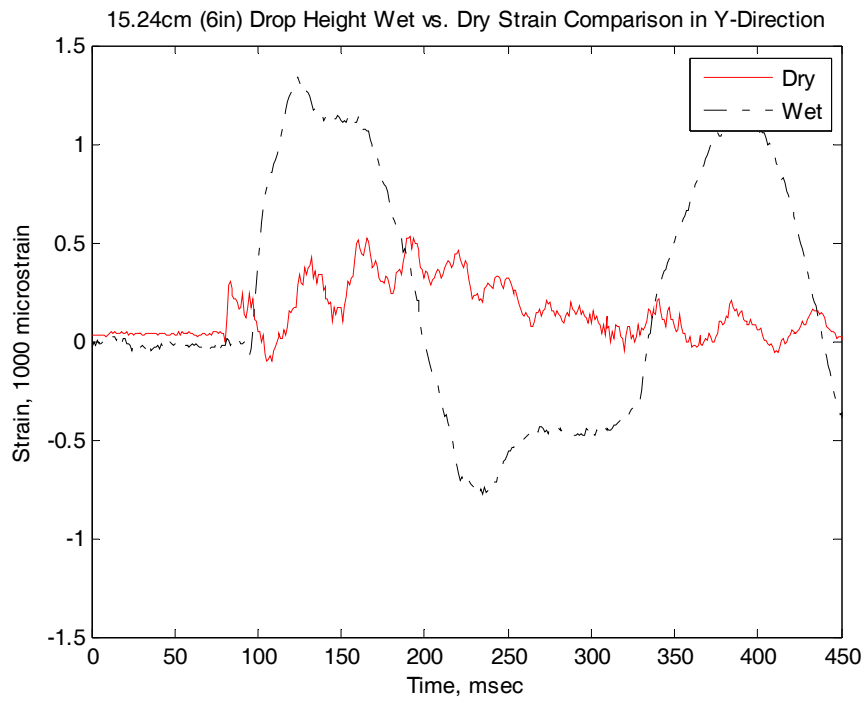


Figure 32. Strain along y-direction at strain gage 2.

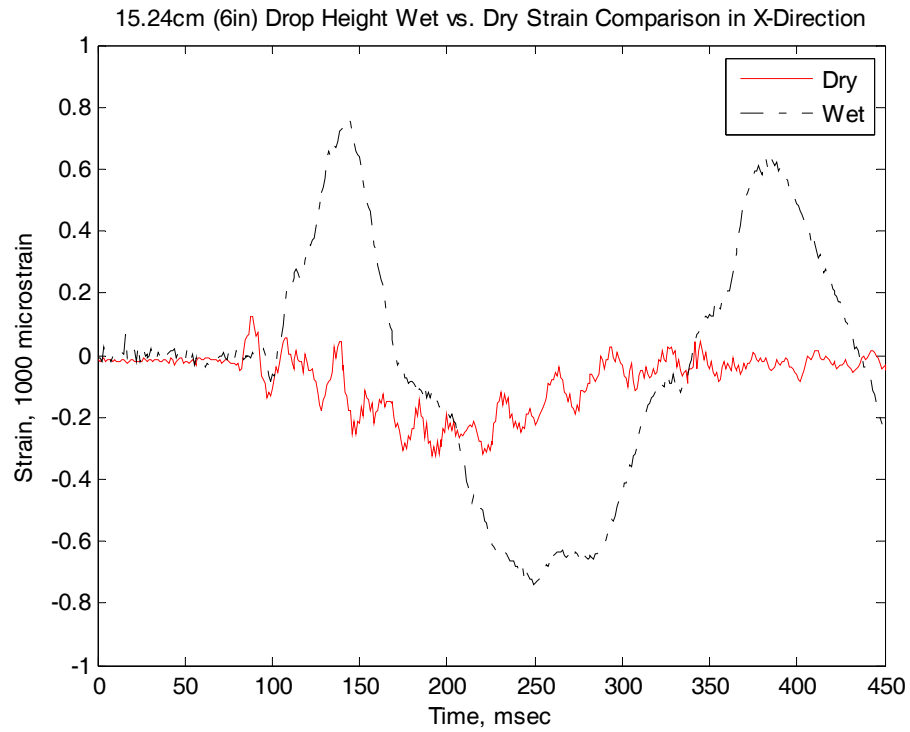


Figure 33. Strain along x-direction at strain gage 3.

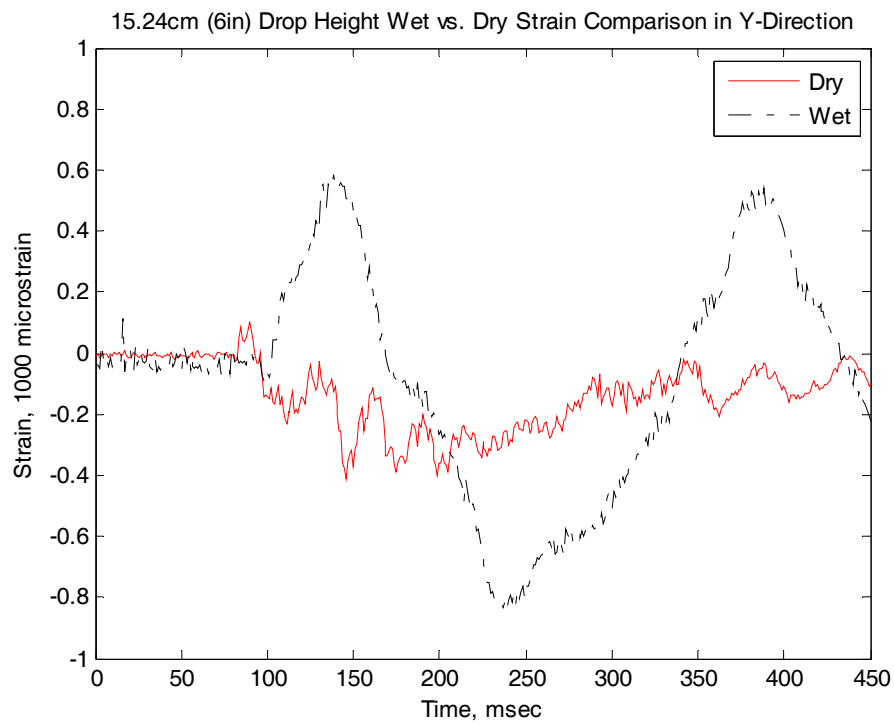


Figure 34. Strain along y-direction at strain gage 3.

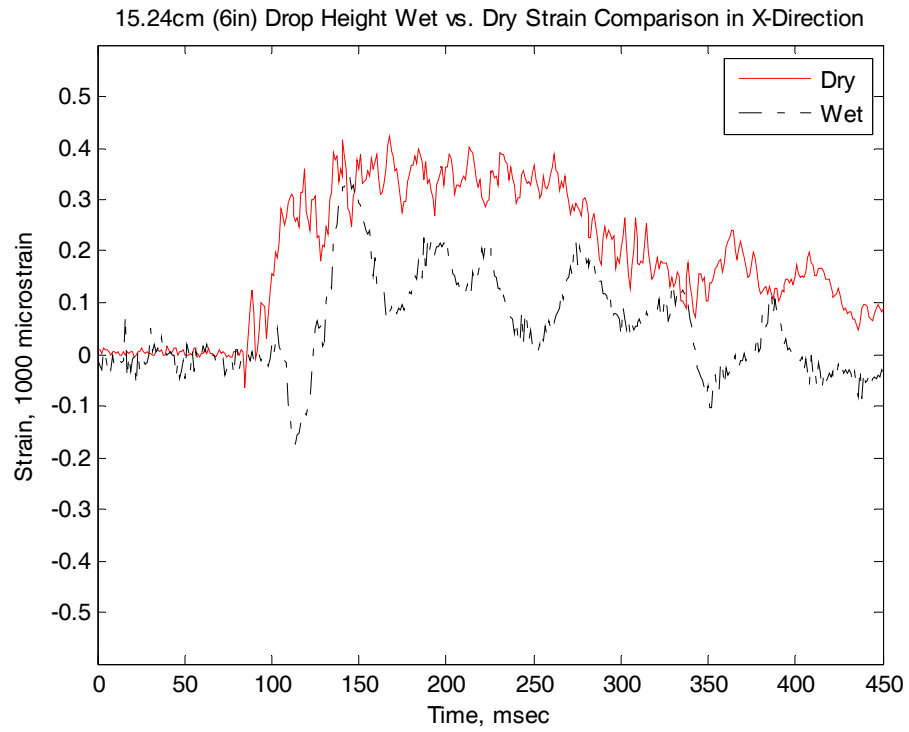


Figure 35. Strain along x-direction at strain gage 4.

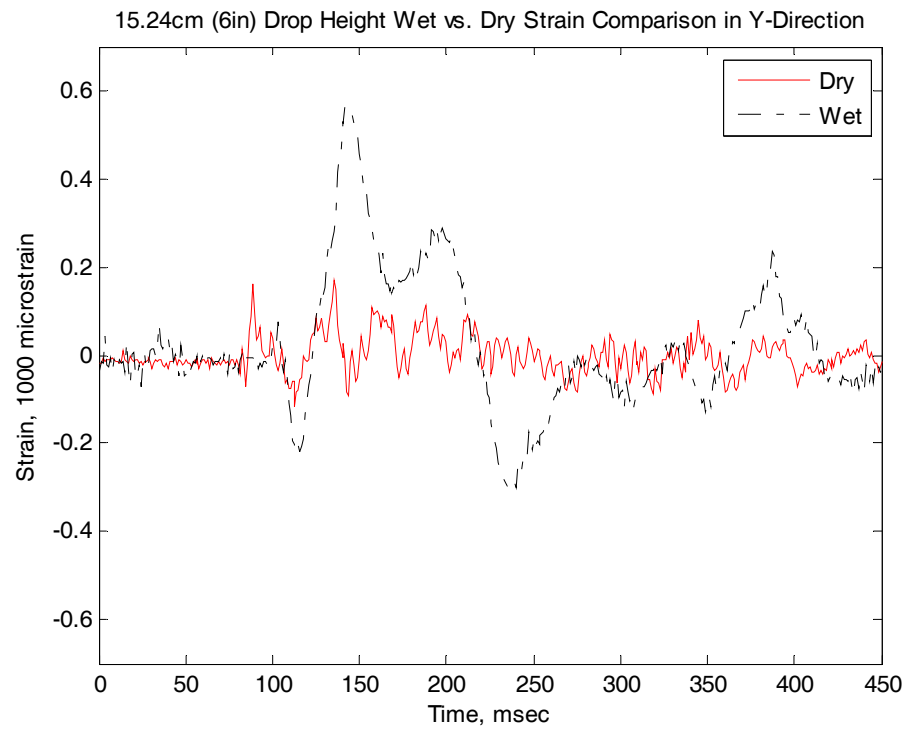


Figure 36. Strain along y-direction at strain gage 4.

Figures 29 through 36 show the strain results for all four strain gages along both the x-direction and y-direction at the 15.24 cm (6 in) drop height. As can be seen at each strain gage the magnitude of the wet composite sample is greater than the dry in all cases. It varies among the four strain gages, but this is due to the proximity of each strain gage to the clamped boundary conditions. This suggests that the FSI effect is not uniform over the composite plate. All of the strain gages show a clear difference among all the response frequencies which can be attributed to the added mass effect and their respective locations in relation to the clamped boundary conditions.

B. CARBON FIBER REINFORCED POLYMER COMPOSITE

1. Overview

The data collected during the impact testing was analyzed in two different ways. First, the force and strain data was plotted to determine the consistency of the data. Since the data from 4 tested samples was very similar, it was concluded that the data was reliable. The data was plotted showing the force and strain results of three samples at the same drop heights. It was then plotted showing the force and strain results of the each sample at the different drop heights. This showed the increase in strain and force as the drop heights increased.

Once the testing was complete, the data was compared to the data collected by Tan [5]. The purpose of the comparison is not to validate the data collected previously, but to study the FSI and its effect on the CFRP in a fully submerged test environment and compare it to the dry test environment.

2. Force Analysis

The force data for the CNT reinforced joint samples is shown in Figures 37 and 38. The data shown is relatively clean and it shows the consistency between each sample. The consistency of the data tells us that the data is reliable and it allowed for the removal of any outliers in the data collection.

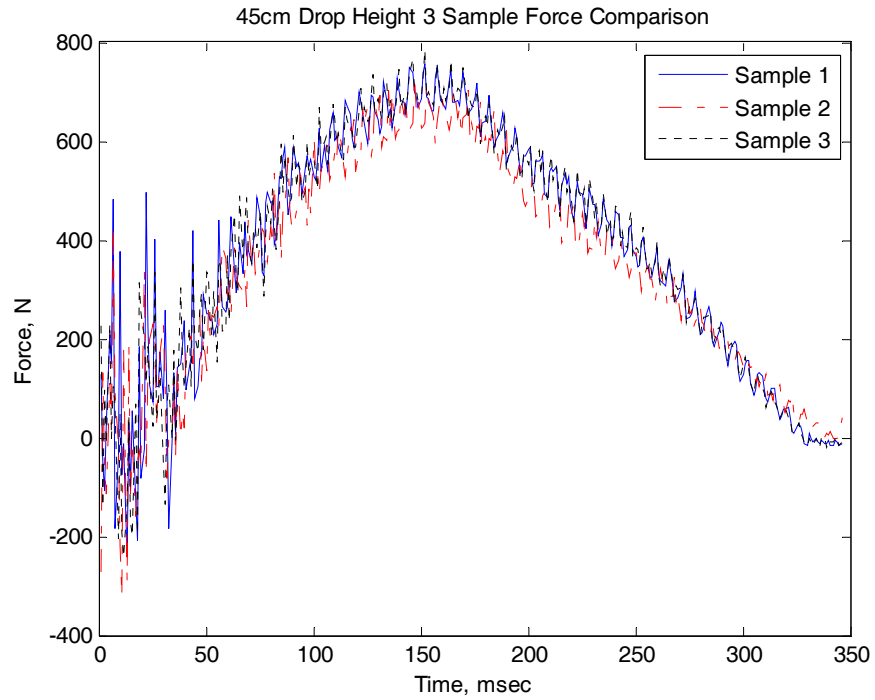


Figure 37. CNT reinforced impact force plot for 45 cm drop height.

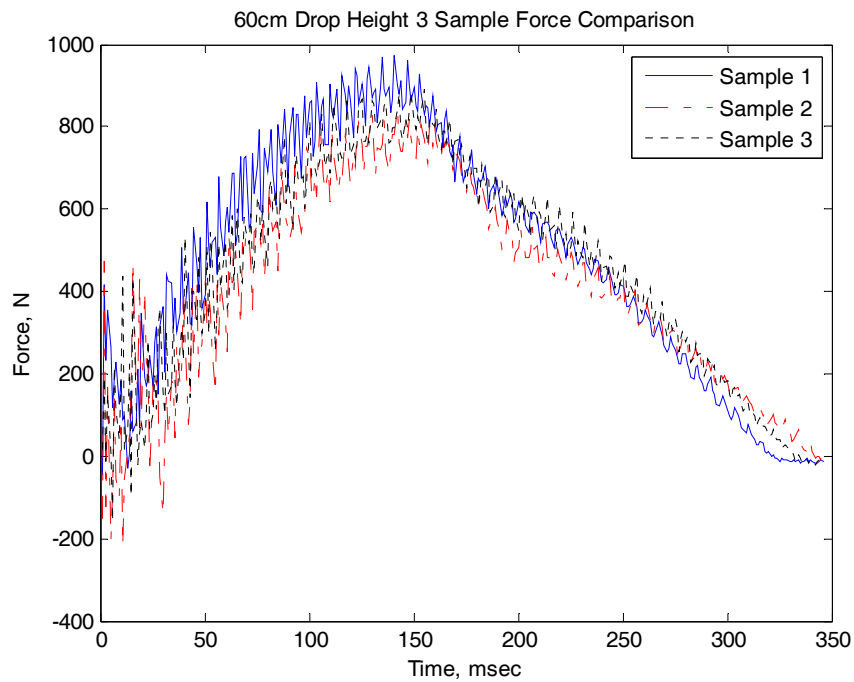


Figure 38. CNT reinforced impact force plot for 60 cm drop height.

Figures 37 and 38 show the impact force plots for the 45cm and 60cm drop heights for samples 1, 2, and 3. These two plots show the consistency of the data and they also show an increase in force as the drop height increases. This is what is expected. To determine the effect of the FSI on the composite samples the data much be compared to the data collected by Tan [5] in his study of the same composite samples using the same test methods.

The data from the dry testing is shown in Figure 39. It shows the gradual increase in force as the drop height is increased for one of the composite samples at three different drop heights.

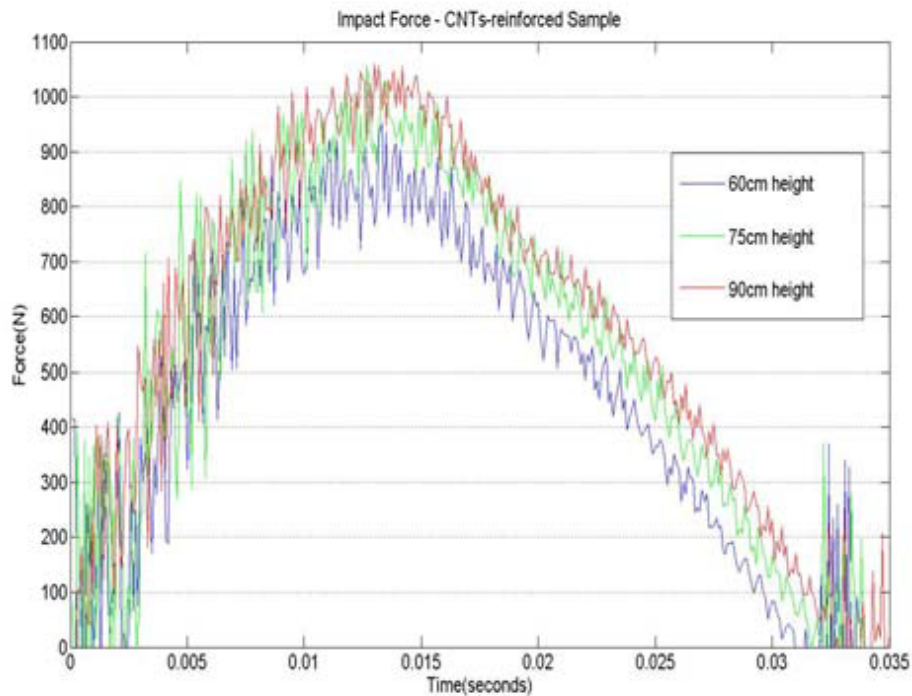


Figure 39. CNT reinforced drop height comparison of dry test [5].

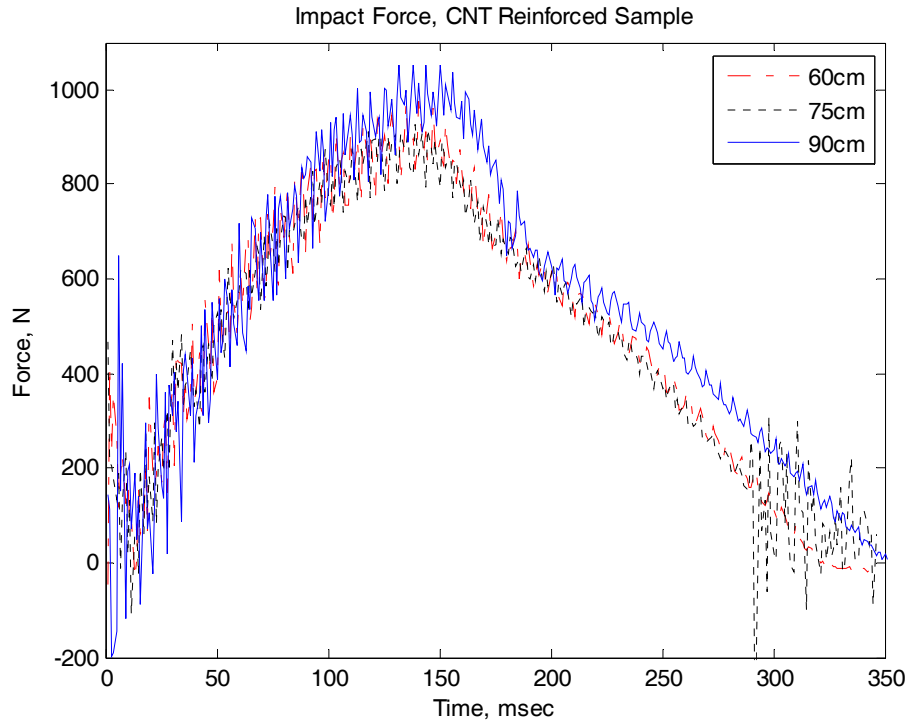


Figure 40. CNT reinforced Sample 1 drop height comparison of impact force for submerged test.

Figure 40 is from the data collected during the submerged testing done for this research. Due to the FSI we would expect the impact force in the submerged testing to be higher than the impact force experienced during the dry testing. However, if Figures 39 and 40 are compared side by side they look very similar except for the fact that the backside of the curves from the dry testing are relatively smooth while the wet testing has a distinct knee, or bend, in the backside of the curve. We know from inspection that a knee in the force data like this one indicates crack propagation. There is no significant increase seen in impact force in the submerged test because of the damage incurred by the sample. Once damage is incurred, there is little difference seen between the force data for the wet and dry test samples. Since no significant increase is shown, the other 2 composite samples data was plotted to compare as well.

After analyzing all three of the CNT samples tested in water and comparing the data to the CNT samples tested in air, it seems clear that FSI played a large role. This can be seen on each of Figures 41 through 43 where there is a significant knee on the

recovery side of the curve. This did not occur in the dry testing until a drop height of 105cm or greater. Here in the submerged testing it consistently occurred at a drop height of 90cm. As stated by Tan [5], a failure was defined as crack propagation very near to the center of the composite sample. It is very difficult to see with the naked eye exactly how far the crack propagated, but the data indicates significant growth.

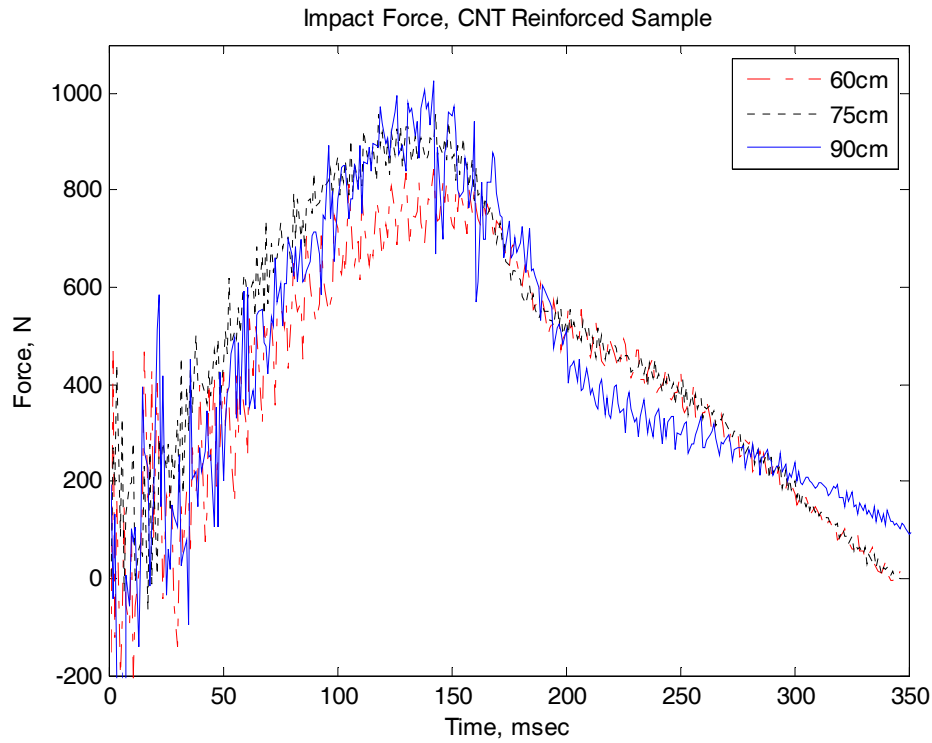


Figure 41. CNT reinforced Sample 2 comparison of impact force for submerged data.

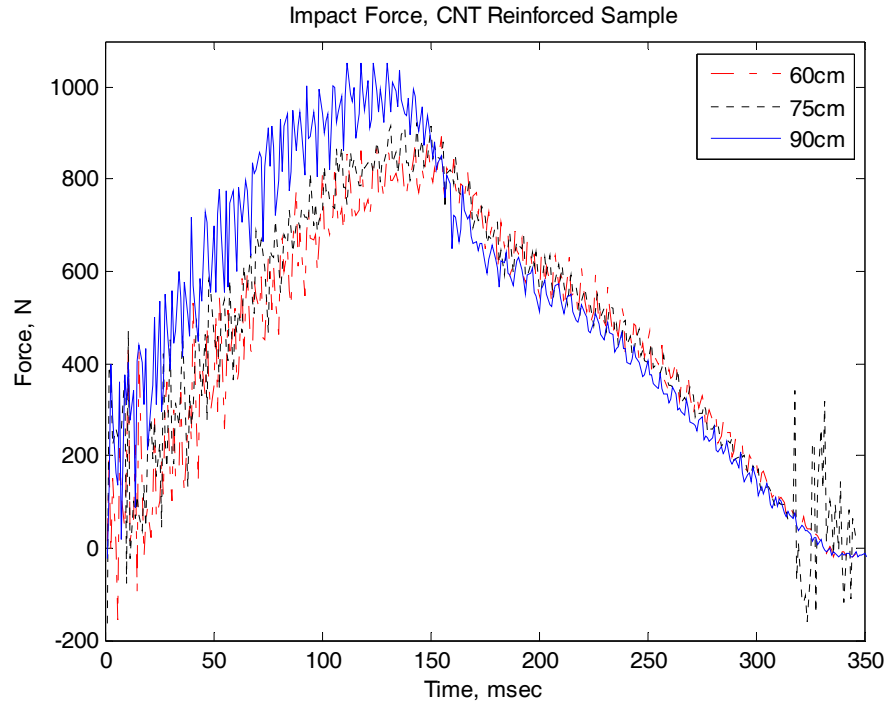


Figure 42. CNT reinforced Sample 3 comparison of impact force for submerged data.

As Figures 40, 41, and 42 show there is no significant increase in impact force for any of the three samples when compared to Figure 39, again, this is due to crack propagation in the joint. Next, a comparison of the non-reinforced joint samples was done.

The non-reinforced data from Tan [5] is presented here in Figure 43. Again it shows the impact forces for three different drop heights of the 2kg weight. It shows a very slight increase in impact force with an increase in drop height, but it is relatively small. The submerged test results can also be seen starting with Figure 44. The data shows similar results to that of the dry testing, but there is a much more distinct increase in impact force with increase of drop height seen in the submerged testing. Sample 1 results shown in Figure 44 have an impact force of approximately 800 N which is slightly more than the impact force for the dry test which shows approximately 750 N. There is a much larger difference as the drop heights increase. For the submerged test, at a 75 cm drop height the impact force is about 925 N compared to 825 N in the dry test.

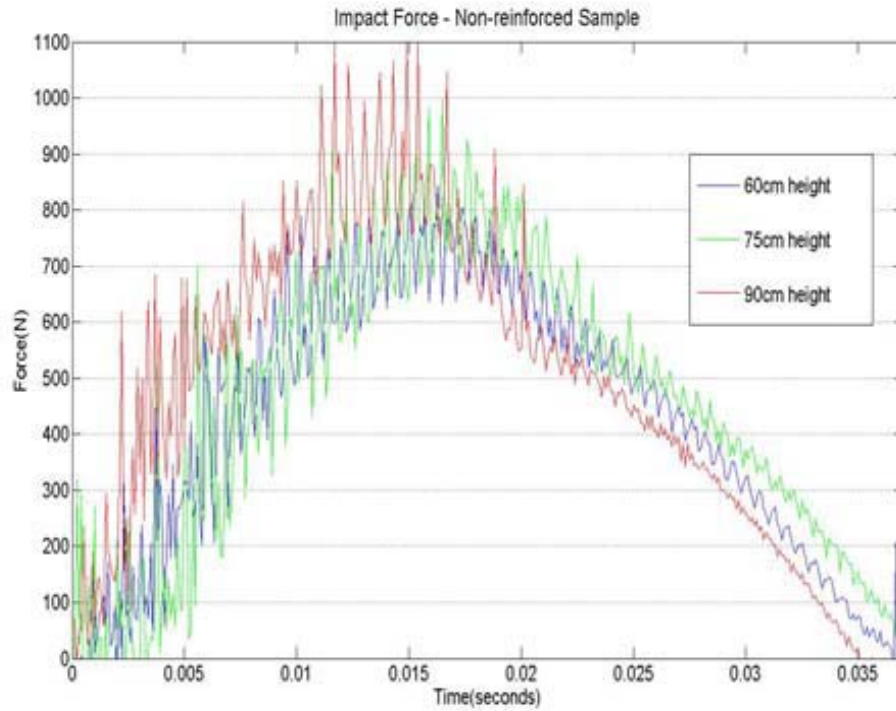


Figure 43. Non-reinforced drop height comparison of impact force for dry test.

The results for Sample 1 of the submerged testing are in Figure 44 and it shows the gradual increase in impact force. It also shows that the overall impact force experienced was greater than that of the dry test sample. This can also be seen in the other two samples tested shown in Figures 45 and 46.

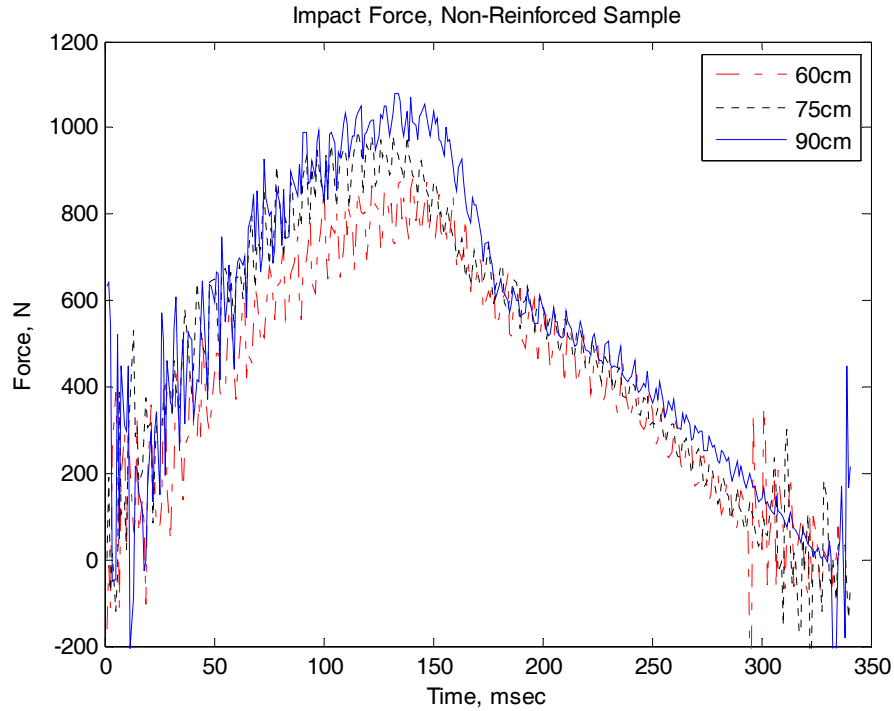


Figure 44. Non-reinforced Sample 1 comparison of impact force for submerged test.

The FSI seems to play a larger role in the non-reinforced joint interface samples. The results are what we expect to see in test like this. Since all of these samples have a density similar to water, the added mass effect of the water during impact should play a larger role. If a drop height of 90 cm from Sample 1 is compared to the 90 cm drop height of the dry test sample, there is about a 200 N increase in impact force. These results were obtained in approximately 30.48 cm (12 in) of water, so it is clear that a small amount of water has a large effect on the composites.

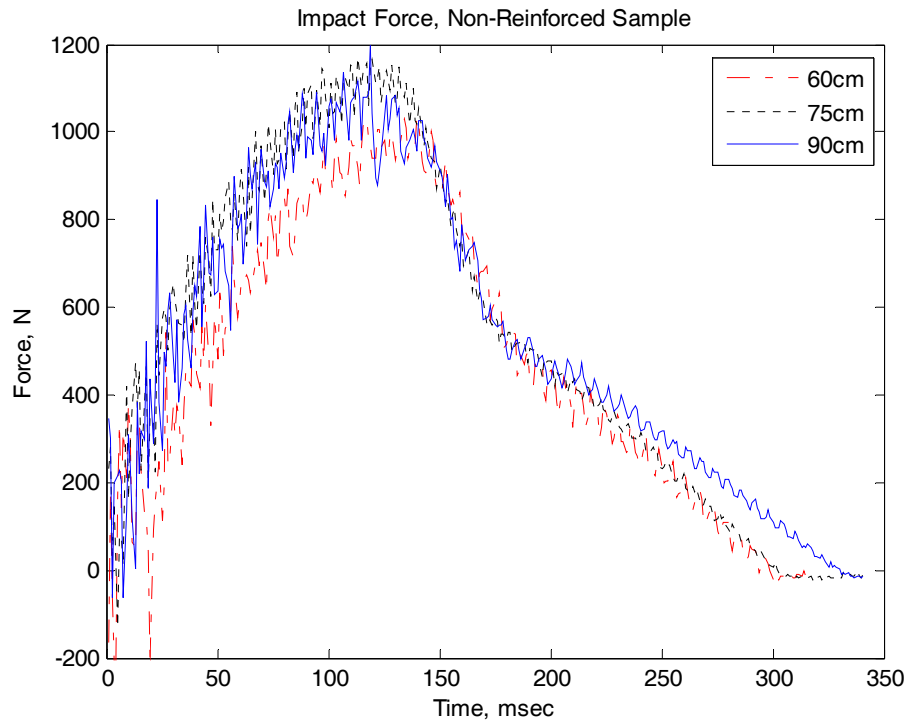


Figure 45. Non-reinforced Sample 2 comparison of impact force for submerged test.

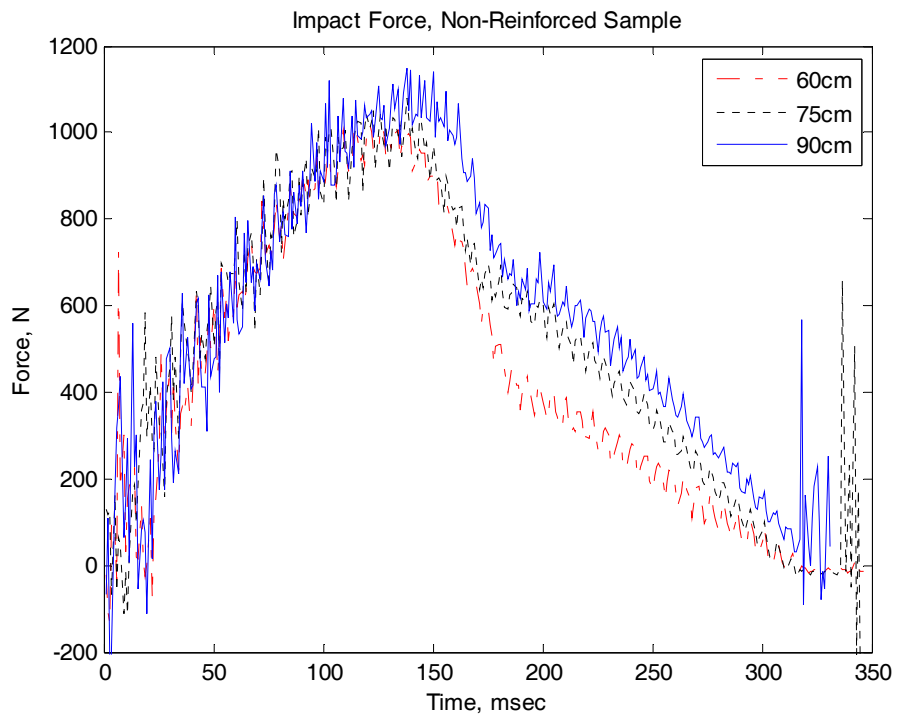


Figure 46. Non-reinforced Sample 3 comparison of impact force for submerged test.

3. Strain Analysis

The CFRP samples only used one strain gage per sample because we were only concerned with what was happening locally at the impact point in the two different test environments. The longitudinal strain was analyzed during this study because the transverse strain would have less of an effect on the joint interface being studied. Figure 47 shows the strain plots from the dry testing of the CNT reinforced joint samples. It shows a very consistent set of data until the 105 cm drop height where a failure occurred. It shows a small, but steady increase in magnitude as the drop height increases.

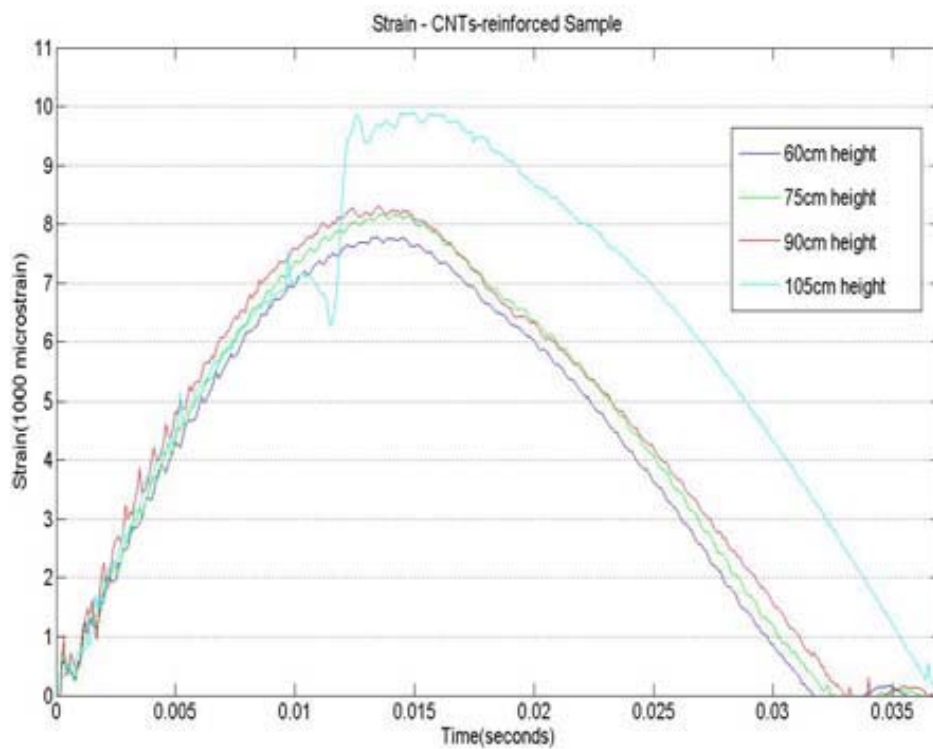


Figure 47. Strain results from dry testing of CNT reinforced joint [5].

The results from the submerged testing of the same samples show very different results. The strain increases significantly for each drop height and in two cases an indication of failure is shown. Figures 48 and 49 show the strain results for two different samples tested during the submerged testing.

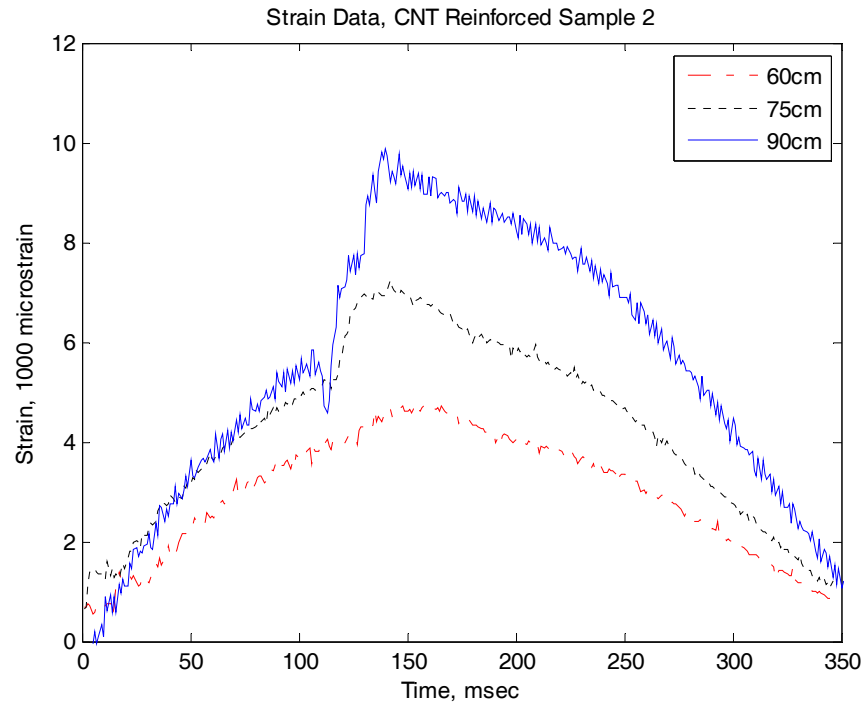


Figure 48. Strain data for submerged CNT reinforced Sample 2.

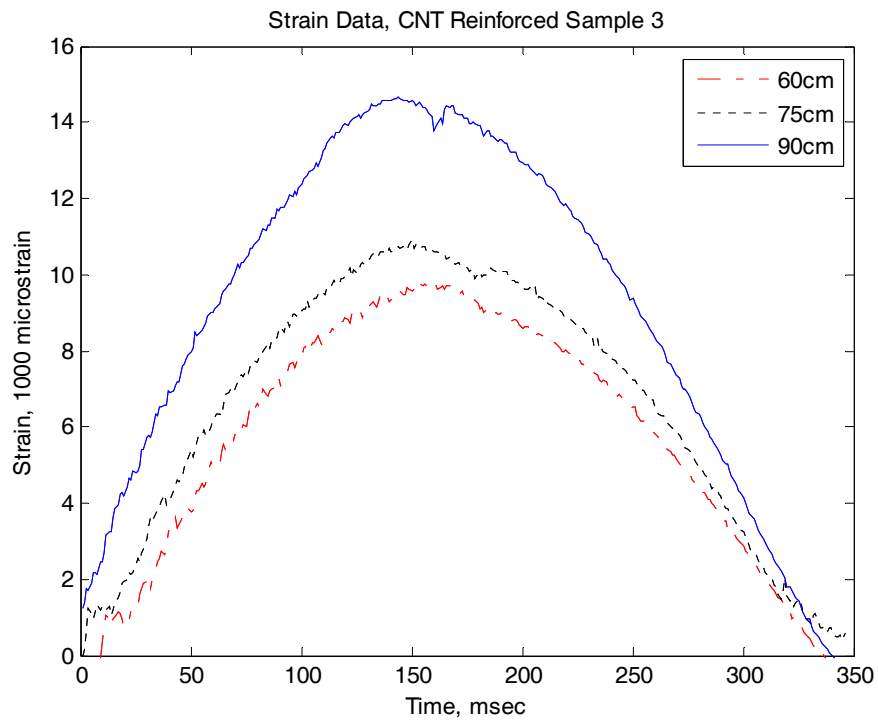


Figure 49. Strain data for submerged CNT reinforced Sample 3.

It can be seen that for each increase in drop height there is a large increase in the magnitude of the strain. Both samples show a very large increase at the 90 cm drop height and in all three cases, the strain at the 105 cm drop height produced a failure in the strain gage readings.

The results from the non-reinforced joint interface in the submerged testing seem to be similar to the results for the dry testing. The data for the dry testing shows small increases in strain for each increase in drop height, which is the same for the submerged testing. The results from the dry testing are shown in Figure 50 and the results from the submerged testing are shown in Figures 51 through 53. The water obviously plays a role here because there is a larger overall strain in the wet tests. However, it was expected that the increase would be larger. It is believed that the reason for such a smaller increase can be attributed to the fact that the impact force plots shown in Figures 43 through 45, all showing a very distinct knee on the backside of the curve. This was discussed earlier as being an indication of failure, or crack propagation. This occurred at drop heights as low as 60 cm. If the CFRP non-reinforced joint samples were experiencing damage from 60 cm on, then the strain would tend to be lower than expected because it is taking less force to propagate the crack further which would relieve some of the strain on each sample. As a result, the data for the non-reinforced joint interface in the submerged tests looks very similar to the results in the dry tests.

The results from the non-reinforced tests also help to further explain the results shown in Figures 48 and 49. It seems that the CNT reinforced joints did what was expected, and CNTs resisted damage and helped to strengthen the joint interface. These results show what we expect to see, and what we expected to see in the non-reinforced data. The strain increases significantly with each drop height and the magnitudes are much higher overall. This shows that the CNTs are doing their job and preventing crack propagation. The strain is much larger because of this.

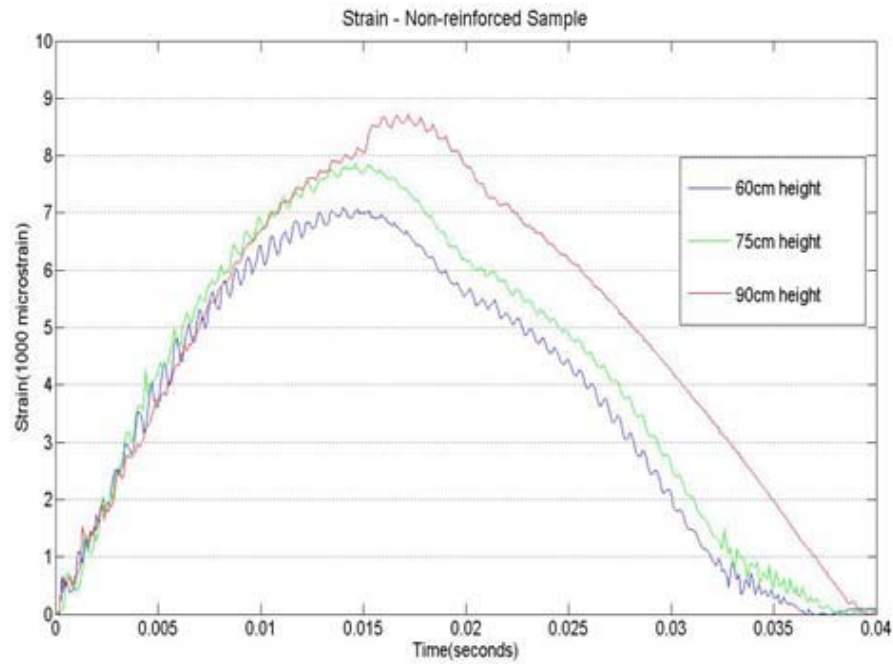


Figure 50. Strain results from dry testing non-reinforced joint [5].

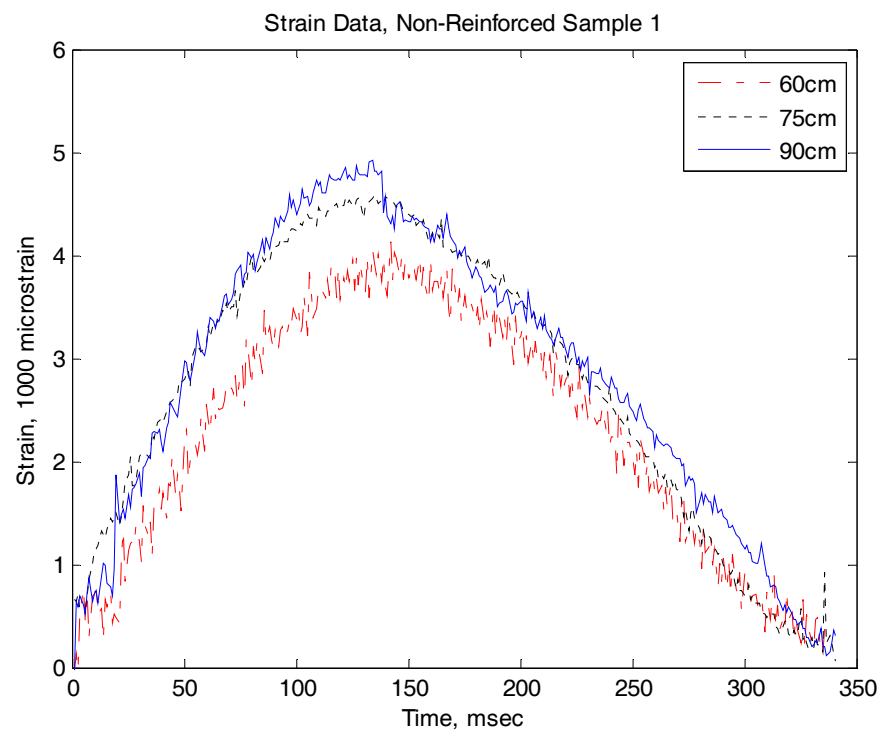


Figure 51. Strain data for submerged non-reinforced Sample 1.

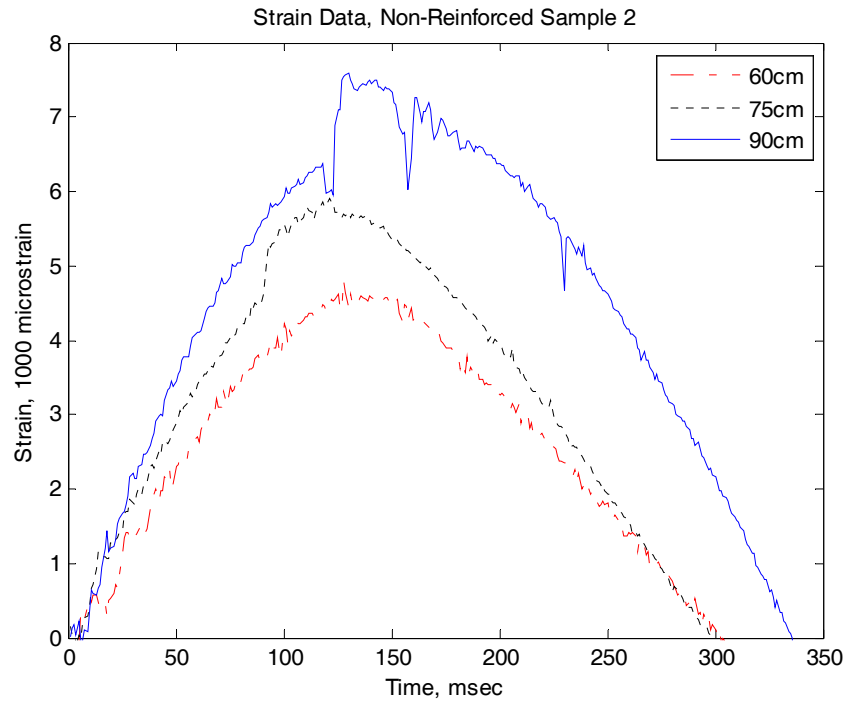


Figure 52. Strain data for submerged non-reinforced Sample 2.

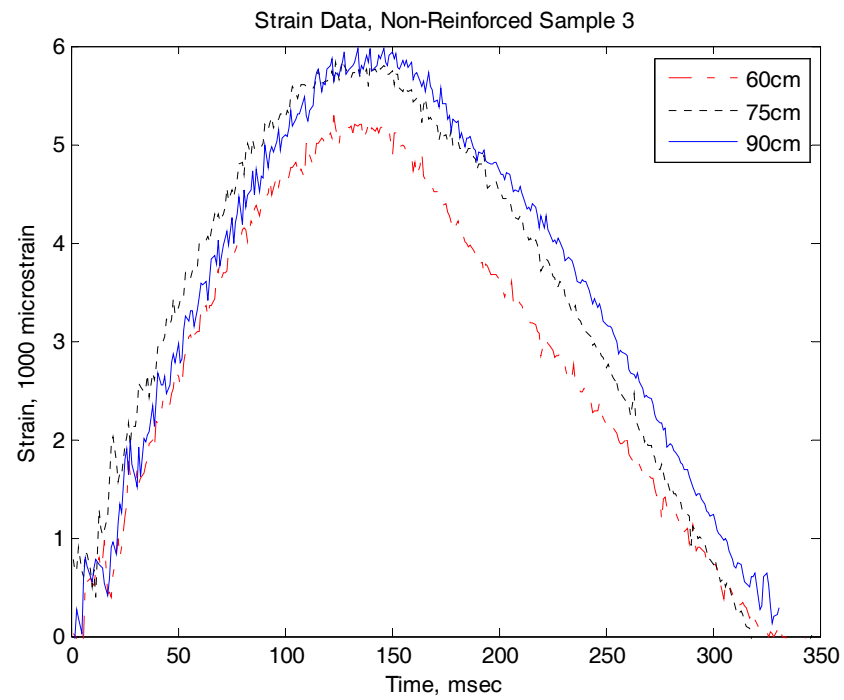


Figure 53. Strain data for submerged non-reinforced Sample 3.

IV. CONCLUSION

This study was done to pursue a better understanding of FSI effects on composite materials made from both a woven fabric E-glass cloth and CFRP, while building upon work that has already been completed. In order to investigate the dynamic response of the composite materials with FSI effects under impact loading, three impact conditions were considered. The conditions were dry, water-backed wet, and water-backed dry. The first two were used to conduct tests on the composite made from the CFRP. The composites made from the E-glass cloth were tested using the dry and water-backed dry test conditions.

Since the composite materials have a very similar density to water, the FSI effects were very significant on the impact force and dynamic response of the plates. Due to the added mass effect of the water, the results for the wet impact test were generally larger than the dry impact tests. As a result, the wet impact was more detrimental to the composite material than the dry impact. It is possible to show a quantitative explanation of the added mass effect by calculating Added Mass Factor. This can be seen in the analysis done by Violette [6]. However, it was discovered that the added mass effect was not uniform over the whole of the plate. This was discovered through the variation of the strain response at each strain gage. The variation was due to the strain gage location in relation to the clamped boundary condition.

It is known that there are many positive effects of CNT reinforcement on strength and fracture toughness. The improvements gained through CNT reinforcement are shown in Ref. [20]. This study sought to gain further knowledge of these effects through testing of pre-cracked composite joints reinforced with CNTs at the crack tip through low velocity impact testing while fully submerged in water and comparing it to the results of non-reinforced joints. The results show that the CNT reinforced samples displayed higher stiffness and experienced failure at higher drop heights than the non-reinforced samples. It clearly showed that introducing CNTs at the crack tip resulted in a resistance to crack propagation. The reinforcement at the joint improved the overall strength of the CFRP samples.

The experimental results show that the dynamic response in a water environment is significantly different than in a dry environment. The impact force experience in water is larger than the force experience in air which led to an earlier onset of damage. The strain deformations clearly show that a water environment will produce larger strains than an air environment. The addition of CNT into the joint interface significantly reduced the crack propagation through the resin.

V. RECOMMENDED FURTHER STUDY

There are still many important aspects of fluid-structure interaction with composites to be studied. One of the more interesting studies would be to take a closer look at the similarities and differences in different types of water based tests. In particular, are the dynamic responses of the fully submerge tests different than the dry top fully submerged tests? How do the damaged incurred compare in each test?

Another study of interest would be to study the modal response and natural frequencies of the composite plates in the different fluid media. This can be done using the high speed camera to capture the response in each fluid media for further analysis.

THIS PAGE INTENTIONALLY LEFT BLANK

LIST OF REFERENCES

- [1] Composite Technology, (2010, January 18). *DDG-1000 Zumwalt: Stealth Warship*. [Online]. Available: <http://www.compositesworld.com/articles/ddg-1000-zumwalt-stealth-warship>.
- [2] B. Griffiths, (2006, August 1). *Rudder Gets New Twist With Composites* [Online]. Available: <http://www.compositesworld.com/articles/rudder-gets-new-twist-with-composites>.
- [3] E.F. Herzberg, "The Annual Cost of Corrosion for DOD," LMI, McLean, VA, Tech. Rep. SKT50T1, April 2006.
- [4] R. Tiron, (2004, July 1). *Navy Gradually Embracing Composite Materials in Ships*. [Online]. Available: http://www.nationaldefensemagazine.org/archive/2004/July/Pages/Navy_gradually3506.aspx
- [5] M.H. Tan, "Effects of Carbon Nanomaterial Reinforcement on Composite Joints Under Cyclic and Impact Loading," M.S. thesis, Dept. Mech. Eng., NPS, Monterey, CA, 2012.
- [6] M. A. Violette, "Fluid Structure Interaction Effect on Sandwich Composites," M.S. thesis, Dept. Mech. Eng., NPS, Monterey, CA, 2011.
- [7] S.D. Faulkner, and Y.W. Kwon, "Fracture Toughness of Composite Joints with Carbon Nanotube Reinforcement," *Journal of Pressure Vessel Technology*, vol. 133, April, 2011. Doi:10.1115/1.4002676.
- [8] US Composite, (2011). *Fiberglass Cloths* [Online]. Available: <http://uscomposites.com/cloth.html>
- [9] Ashland Inc, (2012). *Derakane epoxy vinyl ester resin* [Online]. Available: <http://www.ashland.com/products/derakane-epoxy-vinyl-ester-resin>
- [10] X. Song, "Vacuum Assisted Resin Transfer Molding (VARTM): Model Development and Verification," Ph.D. dissertation, Dept. Mech. Eng., Virginia Tech Univ., Blacksburg, VA, 2003.
- [11] R.D. McCrillis, "Dynamic Failure of Sandwich Beams with Fluid Structure Interaction Under Impact Loading," M.S. Thesis, Mech. Eng., NPS, Monterey, CA. December 2010.

- [12] Vishay Precision Group, (2010, September 12). *Strain Gage Rosettes: Selection, Application and Data Reduction* [Online]. Available: <http://www.vishaypg.com/docs/11065/tn-515.pdf>
- [13] Vishay Precision Group, (2010). *Strain Gage Knowledge Base* [Online]. Available: <http://www.vishaypg.com/ref/straingages>
- [14] A.C. Owens, “An Experimental Study of Fluid Structure Interaction of Carbon Composites Under Low Velocity Impact,” M.S. Thesis, Mech. Eng., Naval Postgraduate School, Monterey, Ca. December 2009.
- [15] W.J. Cantwell and J. Morton, “The significance of damage and defects and their detection in composite materials: a review,” *The Journal of Strain Analysis for Eng. Design*, doi:10.1243/03093247V271029, January 1992.
- [16] T.W. Shyr and Y.H. Pan, “Impact resistance and damage characteristics of composite laminates,” *Composite Struc.* 62, 193–203, 2003.
- [17] W.J. Cantwell and J. Morton, “The impact resistance of composite materials: a review,” *Composites* 22(5), 347–362, 1991.
- [18] S. Abrate, “Impact on laminated composite materials: recent advances,” *Appl Mech. Rev.* 47(11), 517–544, 1994.
- [19] M. W. Richardson and M.J. Wiseheart, “Review of low-velocity impact properties of composite materials,” *Composites* 27A, 1123–1131, 1996.
- [20] Y.W Kwon, A.C. Owens, A.S. Kwon, and J.M. Didoszak, “Experimental Study of Impact on Composite Plates with Fluid-Structure Interaction.” *The International Journal of Multiphysics*, Volume 4 Number 3, 2010.
- [21] V. Kostopoulos, A. Baltopoulos, P. Karapappas, A. Vavouliotis, and A. Paietis, “Impact and after-impact properties of carbon fiber reinforced composites enhanced with multi-wall carbon nanotubes,” *Composites Science and Technology*, vol. 70, pp. 553–563, November, 2009. Doi:10.1016/j.compscitech.2009.023

INITIAL DISTRIBUTION LIST

1. Defense Technical Information Center
Ft. Belvoir, Virginia
2. Dudley Knox Library
Naval Postgraduate School
Monterey, California
3. Professor Young Kwon
Naval Postgraduate School
Monterey, California
4. Research Assistant Jarema M. Didoszak
Naval Postgraduate School
Monterey, California